JCB Journal of Cell Biology

ARTICLE

PP2A-B55 promotes nuclear envelope reformation after mitosis in *Drosophila*

Haytham Mehsen[1], Vincent Boudreau[1,2], Damien Garrido[1], Mohammed Bourouh[3], Myreille Larouche[1,2], Paul S. Maddox[1], Andrew Swan[3], and Vincent Archambault[1,2]

As a dividing cell exits mitosis and daughter cells enter interphase, many proteins must be dephosphorylated. The protein phosphatase 2A (PP2A) with its B55 regulatory subunit plays a crucial role in this transition, but the identity of its substrates and how their dephosphorylation promotes mitotic exit are largely unknown. We conducted a maternal-effect screen in *Drosophila melanogaster* to identify genes that function with PP2A-B55/Tws in the cell cycle. We found that eggs that receive reduced levels of Tws and of components of the nuclear envelope (NE) often fail development, concomitant with NE defects following meiosis and in syncytial mitoses. Our mechanistic studies using *Drosophila* cells indicate that PP2A-Tws promotes nuclear envelope reformation (NER) during mitotic exit by dephosphorylating BAF and suggests that PP2A-Tws targets additional NE components, including Lamin and Nup107. This work establishes *Drosophila* as a powerful model to further dissect the molecular mechanisms of NER and suggests additional roles of PP2A-Tws in the completion of meiosis and mitosis.

Introduction

The roles of kinases in mitosis have been extensively characterized in the past few decades. Cyclin B-CDK1 triggers entry into mitosis (Lindqvist et al., 2009). Phosphorylation of multiple substrates by this enzyme alters their activities to promote chromosome condensation, nuclear envelope (NE) breakdown, and spindle assembly (Morgan, 2007). Other kinases, including Aurora A and Polo, peak in activity when cells enter mitosis and promote this transition (Carmena et al., 2009; Archambault et al., 2015). The onset of chromosome segregation, concomitant with the degradation of mitotic cyclins, marks the beginning of mitotic exit. While some phosphorylated substrates are degraded by the proteasome, thousands of sites on hundreds of proteins are dephosphorylated in an orderly manner during mitotic exit to ensure proper return to G1 (Wurzenberger and Gerlich, 2011; McCloy et al., 2015). Although phosphatases are equally important as kinases, their roles in the cell cycle have been much less studied. Which proteins must be dephosphorylated, at which sites, and by which phosphatases for correct mitotic exit to take place is still poorly understood.

Phosphatases are increasingly recognized as highly regulated and selective enzymes in the coordination of cell division (Rogers et al., 2016). While the number of catalytic phosphatase subunits is inferior to the number of kinases, many phosphatases are regulated by a myriad of associated subunits and posttranslational modifications. The trimeric protein phosphatase 2A (PP2A) is composed of a catalytic subunit C, a scaffold subunit A, and a regulatory subunit B (Wlodarchak and Xing, 2016). Several alternative types of B subunits, generally termed B, B′, B″, and B‴, can modulate PP2A by conferring substrate specificity and directing PP2A to different subcellular locations. In vertebrates, four subtypes of B-type subunits coexist: B55α, β, γ, and δ. B55α and B55δ are ubiquitously expressed and have been shown to play important roles in cell division. PP2A-B55 enzymes efficiently dephosphorylate CDK substrates (Mayer-Jaekel et al., 1994; Castilho et al., 2009; Mochida et al., 2009). In *Xenopus laevis*, depletion of B55δ from interphase egg extracts accelerates mitotic entry (Mochida et al., 2009). In human cells, silencing B55α delays nuclear envelope reformation (NER) and chromosome decondensation and interferes with spindle function in cytokinesis (Schmitz et al., 2010). Genetic work in mice has provided evidence for functions of B55α and B55δ in mitotic exit (Manchado et al., 2010). In *Drosophila melanogaster*, the sole B-type PP2A subunit is encoded by *twins* (*tws*). Mutations in *tws* are lethal and lead to anaphase defects in larval neuroblasts (Mayer-Jaekel et al., 1993). Thus, PP2A-B55 plays an important role in mitotic exit in vivo across animal species.

[1]Institute for Research in Immunology and Cancer, Université de Montréal, Montréal, Québec, Canada ; [2]Département de biochimie et médecine moléculaire, Université de Montréal, Montréal, Québec, Canada; [3]Department of Biology, University of Windsor, Windsor, Ontario, Canada.

Correspondence to Vincent Archambault: vincent.archambault.1@umontreal.ca; Vincent Boudreau and Paul S. Maddox's present address is Department of Biology, University of North Carolina at Chapel Hill, Chapel Hill, NC.

https://doi.org/10.1083/jcb.201804018

PP2A-B55 activity is cell cycle regulated, low in early mitosis and high in late M phase and interphase (Mochida et al., 2009). This regulation depends on Greatwall (Gwl) kinase, which is activated by CDK1 at mitotic entry and phosphorylates Endosulfine proteins (ENSA and Arpp19 in vertebrates, Endos in *Drosophila*). Once phosphorylated by Gwl, Endosulfines act as selective competitive inhibitors of PP2A-B55 (Gharbi-Ayachi et al., 2010; Mochida et al., 2010; Rangone et al., 2011). Endosulfines are substrates of PP2A-B55 that have very high affinity for the enzyme but are dephosphorylated inefficiently, transiently inhibiting PP2A-B55 with respect to its other substrates (Williams et al., 2014). This inhibition of PP2A-B55 promotes the phosphorylation state of CDK1 substrates. At mitotic exit, PP1 initiates Gwl inactivation (Heim et al., 2015; Ma et al., 2016). Endosulfines are eventually dephosphorylated by PP2A-B55, which then becomes active toward other substrates (Williams et al., 2014). The delay between Cyclin B-CDK1 inactivation and PP2A-B55 activation allows an orderly sequence of events in mitotic exit in human cells, with PP2A-B55 acting only after chromosome segregation (Cundell et al., 2013).

PP2A-B55 regulates spindle function in cytokinesis and promotes chromosome decondensation and NER (Schmitz et al., 2010; Cundell et al., 2013; Afonso et al., 2014). However, the important substrates of PP2A-B55 in these functions, and the mechanistic impact of their dephosphorylation are largely unknown. The reassembly of interphase nuclei after mitosis is an orderly process that requires the reconstruction of a NE around chromatin (de Castro et al., 2016; Schellhaus et al., 2016; LaJoie and Ullman, 2017). Proteins of the nuclear lamina and nuclear pores are assembled in a step-wise manner on chromatin-binding adaptors, including barrier-to-autointegration factor (BAF). In *Caenorhabditis elegans*, BAF recruitment to reassembling nuclei has been shown to depend on PP2A, although the mechanism of this regulation is still unclear (Asencio et al., 2012). Little is known about the mechanisms of NER in *Drosophila*.

In this study, we have used *Drosophila* to search for essential functions of PP2A-B55/Tws in the cell cycle. We conducted a maternal-effect genetic screen to identify enhancer mutations of a partial loss of PP2A-Tws function. We hypothesized that we would identify factors that function with PP2A-Tws in mitotic exit as an entry point toward a better mechanistic understanding of this process. We found genetic interactions that pointed toward an important role of PP2A-Tws in NER. We followed up with functional and biochemical studies to dissect the roles of PP2A-Tws in NER. Our results suggest that PP2A-Tws dephosphorylates multiple proteins, including BAF and Lamin, to promote the reassembly of nuclei after mitosis.

Results

A maternal-effect genetic screen for interactors of PP2A-Tws

To identify genes that collaborate with PP2A-Tws in the cell cycle, we conducted a genetic screen in *Drosophila*. We exploited the fact that female meiosis and the first embryonic cell cycles are sensitive to genetic alterations in the cell cycle machinery. Oogenesis and early embryogenesis rely on maternally deposited mRNAs and proteins (Fig. 1 A). Several genes that encode cell cycle regulators or effectors were identified from maternal-effect lethal mutants (Glover, 1989). We used flies that are heterozygous for a strong hypomorphic allele of *tws* (*tws*^{P}) (Uemura et al., 1993). These flies are viable and fertile but are sensitized to partial loss of function in genes that collaborate with PP2A-Tws. We hypothesized that genes of which the loss of a single allele is maternal-effect synthetic lethal in the *tws*^{P}/+ background may function in a common mechanism with PP2A-Tws in the cell cycle (Fig. 1, B and C). Similarly, we previously identified mutations in *tws* as heterozygous enhancers of *gwl*^{Scant}, which encodes a constitutively active form of Gwl, a kinase that antagonizes PP2A-Tws (Wang et al., 2011).

We screened through a collection of deletions on the second and third chromosomes, mostly obtained from the Drosdel isogenic deficiency kit (Ryder et al., 2007). Most of them are large genomic deletions, and together they cover nearly 70% of the genome. Each line was crossed with the *tws*^{P}/*TM6B* line to generate *Df*/+, *tws*^{P}/+ females that were subjected to fertility tests. Deletions that, when combined with *tws*^{P}, resulted in a hatching rate below 50% were selected for further analysis. In parallel to the screen against *tws*^{P}, we similarly screened against a null allele of *microtubule star* (*mts*$^{XE\text{-}2258}$), which encodes the catalytic subunit of PP2A (Wassarman et al., 1996). The genetic interactors of *tws* and *mts* overlapped only partially, suggesting that the mutant allele in *mts* also sensitizes eggs or embryos in PP2A-dependent functions that rely on regulatory subunits other than Tws. Not surprisingly, deletions uncovering *mts* interacted with *tws*, and deletions uncovering *tws* interacted with *mts*, probably because halving the levels of both Tws and Mts simultaneously further compromises the levels of PP2A-Tws holoenzyme. An overview of the primary results is shown in Fig. 1 D. The complete dataset is presented in Table S1.

Finer mapping with overlapping deletions, followed by the testing of candidate genes included in the uncovered genomic intervals, led us to the identification of individual genes for which mutation of one allele in combination with one mutant allele of *tws* or *mts* strongly decreases the viability of embryos in a maternal effect (Fig. S1 A). As expected, we recovered an interaction between *tws* and *polo*, which encodes a mitotic kinase, as previously found (Wang et al., 2011). A strong interaction was found between *tws* and *CycB3*, which encodes the mitotic Cyclin B3, required for anaphase (Yuan and O'Farrell, 2015). Interestingly, we also found interactions between *tws* and *lamin* (*lam; Dm*$_0$), which encodes the Lamin protein, a structural component of the nuclear lamina, around which the NE is assembled during mitotic exit (Schellhaus et al., 2016).

Eggs and embryos with reduced PP2A-Tws and Lamin incur NE defects and abort development

We hypothesized that the genetic interaction between *tws* and *lamin* might reflect a role of PP2A-Tws in NER during mitotic exit. To confirm the genetic interaction between *tws* and *lamin*, we tested different alleles of both genes. Three hypomorphic alleles of *tws* were tested, and all of them enhanced alleles of *lamin* in the following strength order: *tws*^{aar1} > *tws*^{P} > *tws*^{aar2}. Reciprocally, all three alleles of *lamin* tested enhanced alleles of *tws* in the following strength order: *lam*^{K2} ≈ *lam*^{A25} > *lam*^{04643} (Fig. 2 A).

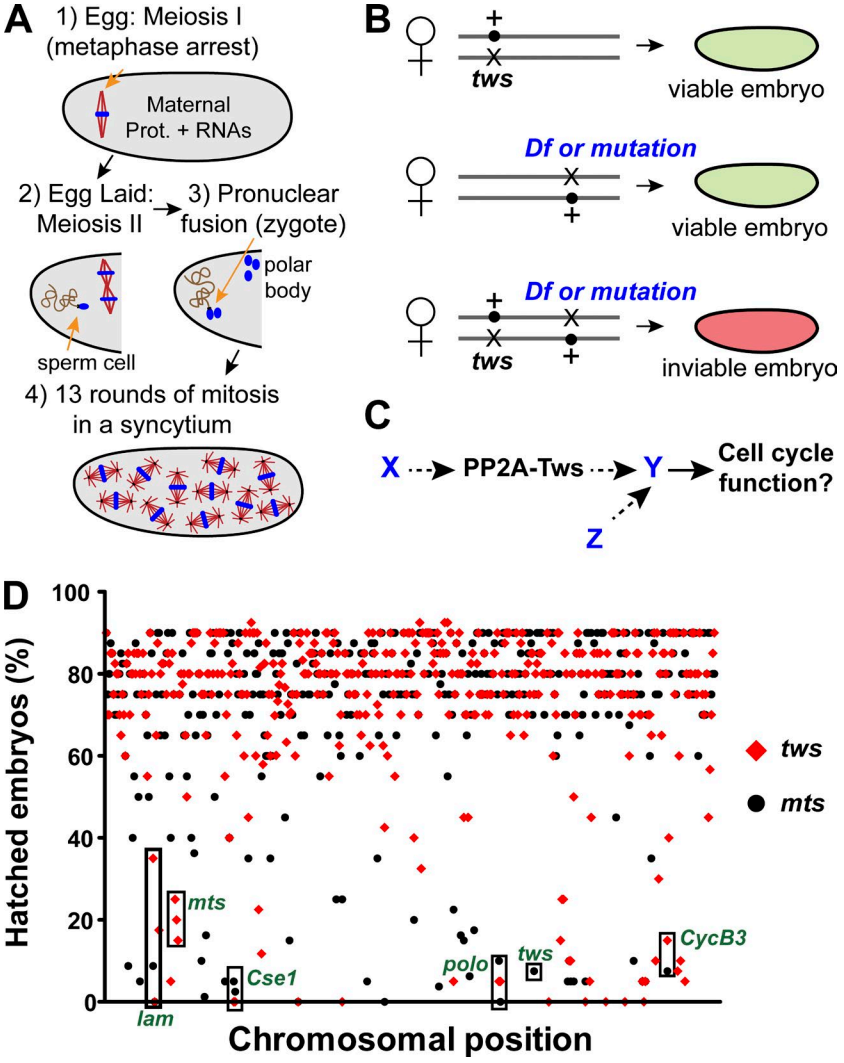

Figure 1. **A maternal-effect second-site noncomplementation screen for interactors of PP2A-Tws. (A)** Completion of meiosis in the egg and early embryogenesis in *Drosophila* depends on maternally provided mRNAs and proteins. **(B)** Design of the screen. Genetic deletions (deficiencies [*Df*]) were combined with a mutant allele of *tws* (*tws*^{P}) or *mts* (*mts*$^{XE\text{-}2258}$) in one cross. Heterozygosity for either *tws*^{P} (or *mts*$^{XE\text{-}2258}$) or the *Df* (or mutation) allows viability and fertility, but heterozygosity for both results in females whose eggs fail to hatch. **(C)** Genes identified in this screen could function upstream of (X), downstream of (Y), or in parallel to (Z) PP2A-Tws in the cell cycle. **(D)** Overview of primary results. Names of particular genes found to interact genetically with *tws* and *mts* are indicated on data points corresponding to deficiencies that uncovered them.

To begin exploring the cellular basis for the lethality observed, we examined embryos aged between 0 and 2 h from *lam*^{K2}/+; *tws*^{P}/+ mothers. Western blots confirmed that mothers heterozygous for the *tws*^{P} and *lam*^{K2} mutations produced embryos with lower levels of Tws and Lamin (Fig. 2 B). Immunofluorescence revealed that the majority of embryos undergoing mitotic development have severe defects (Fig. 2 C). Nuclei are often mispositioned and have abnormal sizes and shapes. Centrosomes are frequently disjoined from nuclei (quantified in Fig. 2 D). Chromatin masses are seen free in the cytoplasm, often attached to NE fragments, as if shredded. All these phenotypes could result from a weakness or defect in the NE. Time-lapse imaging of syncytial embryos from *lam*^{K2}/+; *tws*^{P}/+ mothers also expressing GFP-Polo as a marker of mitotic structures (Moutinho-Santos et al., 1999) reveals that the disintegration of nuclei/centrosome units leads to further disorganization, including spindle fusions and uneven nuclear spacing (Videos 1 and 2). Embryos laid by *tws*^{P}/+ or *lam*^{K2}/+ mutants displayed only minor developmental defects, such as occasional centrosome detachment from nuclei (Figs. 2 D and S2).

Although major defects are prevalent in *lam*^{K2}/+; *tws*^{P}/+ derived embryos where mitotic nuclei are detected at the cortex, we found that the majority of eggs laid do not reach that stage (Fig. 2 E). We therefore investigated potential earlier defects, as early as meiosis. Normally, an oocyte arrests in metaphase of meiosis I until it is laid by the mother. Ovulation triggers completion of meiosis I, and meiosis II immediately follows with two spindles attached together at one pole. At the end of meiosis II, four haploid nuclei assemble an NE around decondensed chromatin in postmeiotic interphase. If the egg has been fertilized, then the innermost nucleus generally becomes the female pronucleus, and it joins the male pronucleus before the first mitosis occurs. The other three nuclei eventually come together and undergo NE breakdown (NEB), chromatin condenses and associates with a microtubule array as a polar body (Fig. 1 A). If the egg is not fertilized, then all four postmeiotic nuclei assemble into a polar body. We collected eggs/embryos aged between 0 and 20 min and analyzed them by immunofluorescence after fixation using a protocol allowing deep staining. We found *lam*^{K2}/+; *tws*^{P}/+ eggs at all stages of meiosis, with similar frequencies to single mutant eggs (Fig. 3, A–I). However, in eggs from *lam*^{K2}/+; *tws*^{P}/+ mothers, we found that NE structures as detected by Lamin staining were often absent or of irregular shape (Fig. 3, F, G, and J). These results suggest that when levels of PP2A-Tws and Lamin are halved, the assembly of postmeiotic interphase nuclei is compromised.

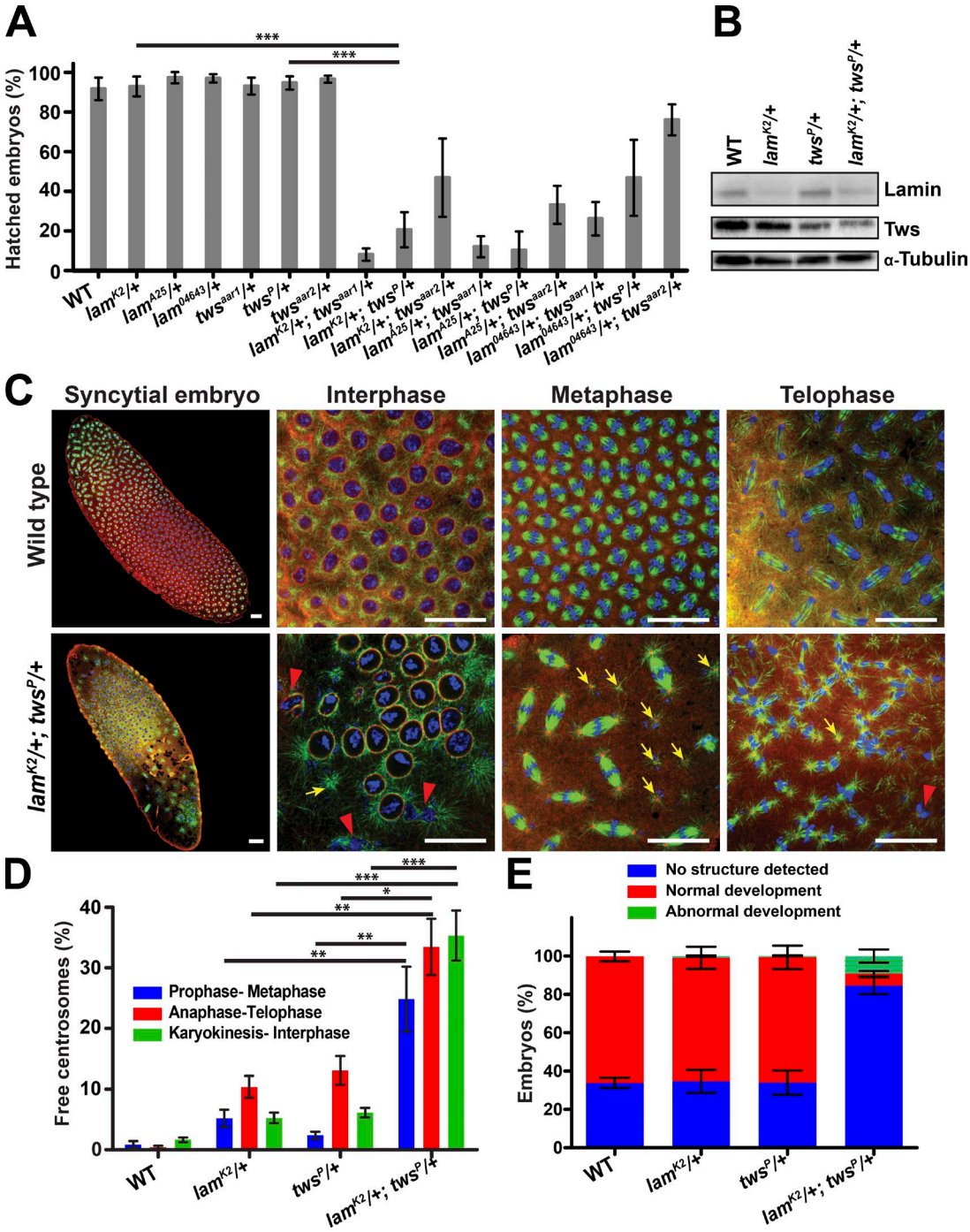

Figure 2. **Collaboration between PP2A-Tws and Lamin is required for syncytial embryonic development. (A)** Genetic interactions between different alleles of *tws* and *lam*. Percentages of hatching of embryos from females of the indicated genotypes were scored. Error bars represent SEM. ***, P < 0.0001, two-tailed *t* test. **(B)** Western blots from embryos showing how protein levels are affected by the maternal genotypes. **(C)** Phenotypes in embryos revealed by immunofluorescence against α-Tubulin (green), γ-Tubulin and Lamin (red), and DNA (DAPI, blue). In embryos from $lam^{K2}/+; tws^{P}/+$ females, several defects are observed: aberrant nuclear distribution (left), interphase nuclei of abnormal shapes and sizes, centrosome detachments (yellow arrows), and broken nuclei (red arrowheads). Scale bars, 20 µm. **(D)** Quantification of free centrosomes observed at different cell cycle stages in embryos of the indicated genotypes. **(E)** Quantification of global embryonic development for the indicated genotypes. Error bars represent SEM. *, P = 0.0165; **, 0.0021 < P < 0.0027; ***, P < 0.0001, two-tailed *t* test.

Using FISH against the X chromosome, we found that most eggs from $lam^{K2}/+; tws^{P}/+$ mothers form a zygotic nucleus containing at least one X chromosome, indicating that a female pronucleus contributed to zygote formation (data not shown). Therefore, while NE formation is compromised, pronuclear apposition can still occur, suggesting that the failure of embryos to develop is due primarily to defects that happen after meiosis in the early mitotic divisions.

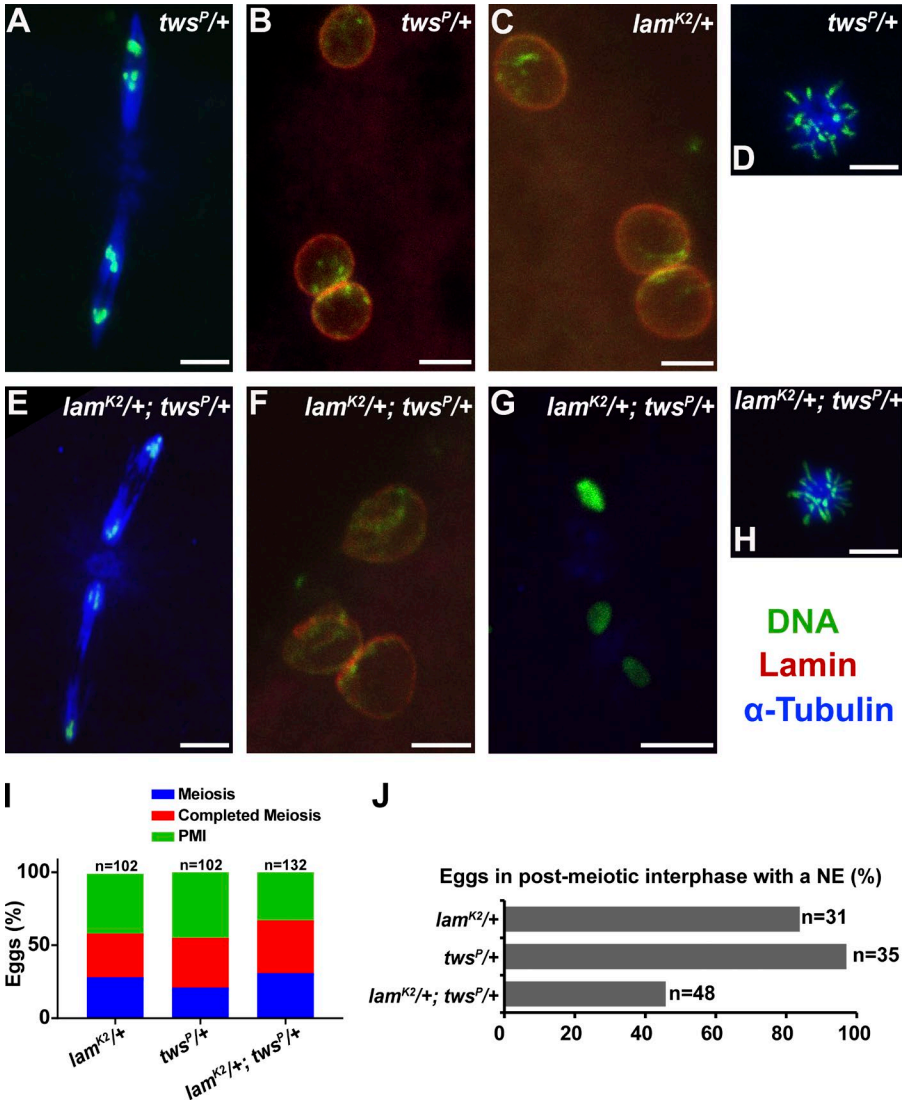

Figure 3. **PP2A-Tws and Lamin cooperate for NER in meiosis.** Eggs were collected for 0 to 20 min, fixed in methanol, and stained for α-Tubulin (blue), DNA (green), and Lamin (red). **(A–D)** Representative images from $lam^{K2}/+$ or $tws^{P}/+$ eggs. **(A)** Meiotic spindles in anaphase II. **(B and C)** Postmeiotic interphase; three nuclei are shown with NEs present around each nucleus. **(D)** A polar body is formed after completion of meiosis. **(E–H)** Representative images from $lam^{K2}/+$; $tws^{P}/+$ double eggs. **(E)** Normal meiotic spindles in anaphase II. **(F and G)** Several $lam^{K2}/+$; $tws^{P}/+$ eggs in postmeiotic interphase show either three nuclei with faint and irregular NEs (F compared with B and C) or three nuclei without NEs (G). **(H)** The majority of eggs from $lam^{K2}/+$; $tws^{P}/+$ mothers are able to complete meiosis normally, indicated by the formation of a polar body. **(I)** Eggs from $lam^{K2}/+$; $tws^{P}/+$ mothers complete meiosis. Phenotypes observed were classified as either in meiosis, in postmeiotic interphase (PMI) or completed meiosis (indicated by the formation of a polar body). **(J)** Quantification of the fraction of eggs in postmeiotic interphase with detectable NEs. For data in I and J, numbers were pooled from two separate stainings and scorings done with eggs cumulated after multiple collections with immediate fixations. Scale bars, 5 µm.

To explore the specificity of the genetic link between Lamin and PP2A-Tws, we tested for potential genetic interactions between lam^{K2} and different mutant alleles of various phosphatase subunits (Table S2). Strong genetic interactions were found only between lam^{K2} and *tws* or *mts* mutant alleles, suggesting that PP2A-Tws plays a particularly important role in relation to Lamin.

CDK phosphorylation consensus sites in Lamin control its solubility

Based on these results, we hypothesized that PP2A-Tws could dephosphorylate Lamin to promote its function at the NE. The regulation of lamins by phosphorylation is complex and not completely understood, but their phosphorylation at CDK sites has been shown to promote lamina disassembly in various systems (Heald and McKeon, 1990; Peter et al., 1990; Machowska et al., 2015). In *Drosophila* Lamin, six of the seven minimal CDK motifs (S/T-P) were so far found to be phosphorylated (Machowska et al., 2015). To begin testing if phosphorylation at CDK sites is required for the dispersal of *Drosophila* Lamin in mitosis, we mutated all seven CDK sites into Ala (7A) or Asp (7D) residues (Fig. 4 A). We then made stable cell lines allowing inducible expression of RFP-$Lamin^{WT}$, RFP-$Lamin^{7A}$, or RFP-$Lamin^{7D}$ and imaged cell division. While RFP-$Lamin^{WT}$ localizes to the NE in interphase, it becomes dispersed throughout the cell in mitosis (Fig. 4 B, top; and Video 3). In contrast, RFP-$Lamin^{7A}$ fails to disperse in mitosis, forming an elongating mass around

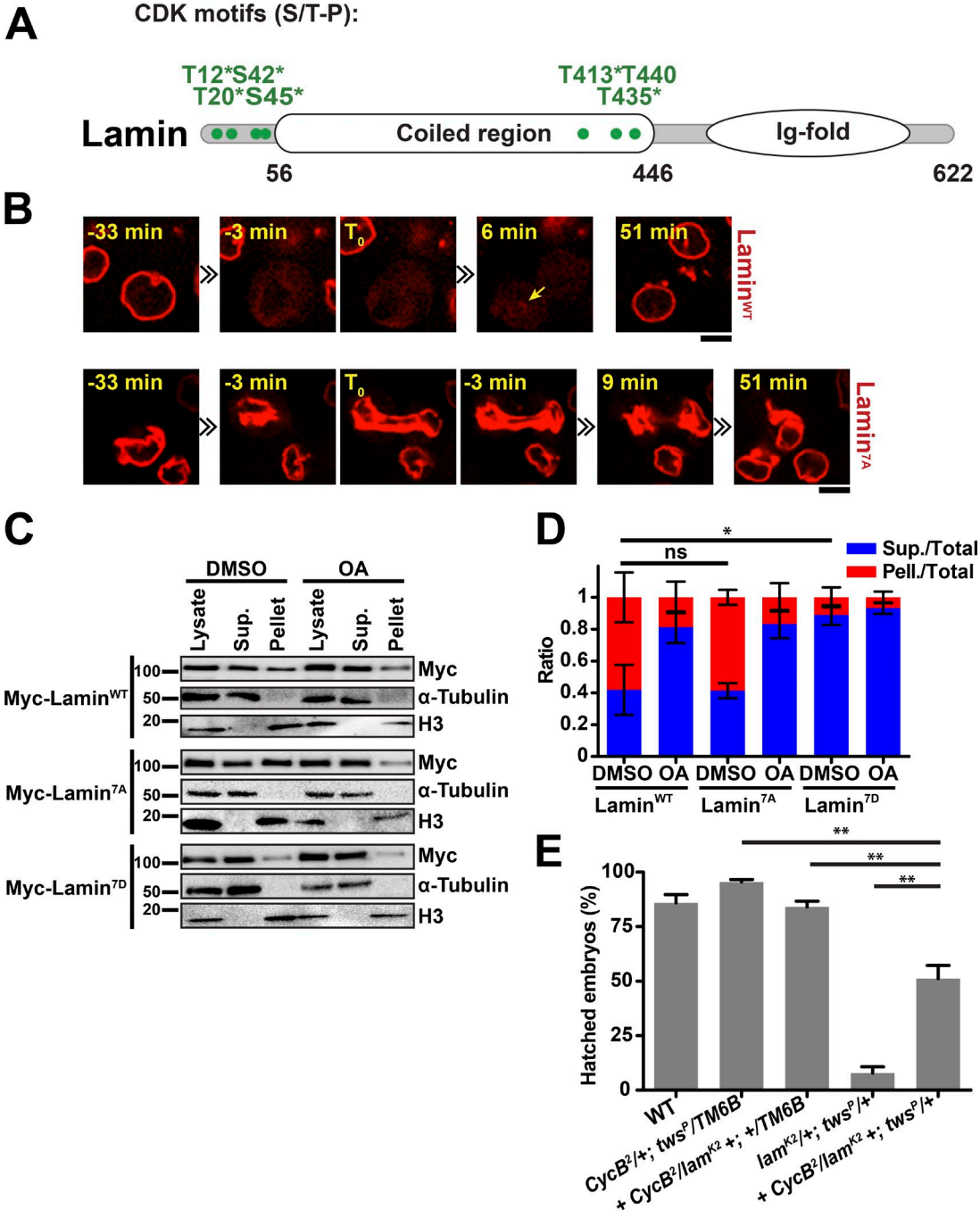

Figure 4. **Phosphorylation at CDK phosphorylation consensus sites in Lamin may promote its dispersion in mitosis. (A)** All seven minimal CDK phosphorylation consensus sites, shown here in a schematic Lamin structure (Lyakhovetsky and Gruenbaum, 2014), were mutated into Ala or Asp residues. Asterisk (*) indicates phosphorylation sites observed experimentally (Machowska et al., 2015). **(B)** Cells expressing RFP-Lamin^{WT} or RFP-Lamin^{7A} were filmed on a spinning-disk confocal microscope. T_0 was defined as the beginning of the cell's elongation as it divides. While RFP-Lamin^{WT} becomes dispersed in mitosis and starts being recruited at 6 min (arrow), RFP-Lamin^{7A} is never dispersed as the cells progress through mitosis. Scale bars, 5 µm. **(C)** Mutation of all CDK consensus sites into Asp in Lamin (Myc-Lamin^{7D}) increases its solubility. Stable cell lines expressing the indicated proteins were treated as indicated before being lysed and the insoluble material was pelleted (see Materials and methods). Fractions were analyzed by Western blot. **(D)** Quantification of relative Western blots signals from soluble and insoluble fractions from three independent experiments as in B. Error bars represent SD. *, P = 0.0437, two-tailed *t* test. **(E)** Introduction of one null allele of *CycB* (*CycB*^{2}) in *Lam*^{K2}*/+; tws*^{P}*/+* females rescues the development of embryos they produce. Percentages of hatching of embryos from females of the indicated genotypes were scored. Error bars represent SD. **, 0.0051 < P < 0.0095, two-tailed *t* test.

the presumptive chromosome mass that is successfully split into two nucleus-like structures as the cell divides (Fig. 4 B, bottom; and Video 4). These results suggest that phosphorylation of Lamin at CDK consensus sites is required for normal dispersion of Lamin in mitosis. However, we observed that RFP-Lamin^{7D} also fails to become dispersed in mitosis (data not shown), possibly because the 7 Asp substitutions do not fully mimic the effect of phosphorylation.

To test biochemically if phosphorylation of Lamin at CDK sites promotes its dispersion in the cell, we made cells expressing the different forms of Myc-Lamin. Cells were lysed and extracts were centrifuged to separate a soluble fraction (supernatant) from an insoluble fraction (pellet) containing the chromatin. Lysates were analyzed by Western blots. While 40% of Myc-Lamin^{WT} is soluble, 80% of Myc-Lamin^{7D} is soluble under these conditions (Fig. 4, C and D). Myc-Lamin^{7A} behaves similarly to Myc-Lamin^{WT} in these extracts from asynchronous cells. These results suggest that phosphorylation at CDK consensus sites in Lamin may disrupt an interaction that promotes lamina assembly. Treating cells with okadaic acid (OA), which inhibits a subset of phosphatases, including PP2A, increased the solubility of Myc-Lamin^{WT}, consistent with the idea that PP2A-Tws promotes lamina assembly (Fig. 4, C and D). However, Myc-Lamin^{7A} was similarly affected by OA, suggesting that phosphorylation outside CDK sites on Lamin can also disrupt the lamina (see below).

Finally, we used genetics to test if Cyclin B-CDK1 antagonizes the collaboration between PP2A-Tws and Lamin in embryos. We found that introduction of a *CycB* mutant allele in *lam^{K2}/+; tws^{P}/+* females partially rescues their fertility, suggesting that PP2A-Tws promotes NER partly by dephosphorylating Cyclin B-CDK1 sites, possibly on Lamin (Fig. 4 E).

PP2A-Tws promotes the recruitment of Lamin and Nup107 to nascent nuclei during mitotic exit

The genetic and biochemical results described above suggested that PP2A-Tws might promote Lamin reassembly on nuclei at the end of mitosis. To test this idea, we generated a *Drosophila* D-Mel2 cell line that stably expresses GFP-Lamin and mCherry-α-Tubulin and examined the effect of Tws depletion by RNAi on the reassembly of GFP-Lamin. Silencing of Tws was confirmed by Western blot (Fig. 5 A). In control cells (transfected with double stranded RNA [dsRNA] against a bacterial kanamycin resistance gene [KAN]), GFP-Lamin starts to enrich on reforming nuclei 5 to 10 min after anaphase spindle elongation. By contrast, in Tws-depleted cells, GFP-Lamin appears later, 20 to 25 min after spindle elongation (Fig. 5, B and C). We conclude that PP2A-Tws promotes the recruitment of Lamin during NER.

We wondered if PP2A-Tws specifically promotes the recruitment of Lamin in NER or if it also affects other components of the NE. We examined Nup107, a component of the Nup107-Nup160 subcomplex whose recruitment at the NE nucleates nuclear pore complex assembly and does not depend on Lamins in human cells (Clever et al., 2012; Schellhaus et al., 2016). Moreover, human Nup107 is phosphorylated in mitosis and is efficiently dephosphorylated by PP2A-B55 (Glavy et al., 2007; Cundell et al., 2016). As for GFP-Lamin, the recruitment of GFP-Nup107 is delayed upon Tws depletion (Fig. 5, D and E). We also tested mutations in *Nup107* and found that they genetically interact with *tws*, like mutations in *lamin*, with similar embryonic phenotypes (Fig. S3). These results could reflect a role of PP2A-Tws in the dephosphorylation of both Lamin and Nup107 to promote their recruitment to the NE. Alternatively, PP2A-Tws could dephosphorylate a factor upstream of both Lamin and Nup107 to promote NER.

PP2A-Tws promotes the recruitment of the upstream factor BAF to nascent nuclei during mitotic exit

In light of the above results, we searched for a protein that could be regulated by PP2A-Tws upstream of Lamin and Nup107 during NER. We became interested in BAF, as its human orthologue may be the first protein to be recruited in the NER cascade (Schellhaus et al., 2016). BAF is a conserved protein that interacts with both DNA and LEM (LAP2-Emerin-MAN1)-domain proteins of the NE in interphase (Margalit et al., 2007). In human cells and *C. elegans*, BAF becomes dispersed in the cytoplasm in early mitosis and is recruited back on DNA in telophase, where it holds chromosomes together, allowing the formation of the NE around a single nucleus (Haraguchi et al., 2001; Samwer et al., 2017). Moreover, the recruitment of BAF to chromatin during telophase has been shown to depend on PP2A in *C. elegans* and HeLa cells, although the identity of the regulatory subunits of PP2A involved is unclear (Asencio et al., 2012).

To examine the dynamics of *Drosophila* BAF in cell division, we made a stable cell line expressing GFP-BAF and mCherry-Tubulin. We found that *Drosophila* BAF is nuclear in interphase and becomes dispersed in the cell in mitosis. During mitotic exit, GFP-BAF is quickly recruited to chromatin, starting 4 min after spindle elongation (Fig. 6, A [top] and B; and Video 5). We tested if this recruitment of BAF depends on PP2A-Tws. Depletion of Tws results in a delay in GFP-BAF recruitment during NER. In addition, the recruitment pattern is altered. In control cells, GFP-BAF is initially strongly recruited on chromosomes while they still appear condensed (early phase), and GFP-BAF then becomes restricted to the nuclear periphery (late phase). Similar dynamics were observed in human cells (Haraguchi et al., 2001, 2008). Instead, in Tws-depleted cells, GFP-BAF recruitment is immediately restricted to the nuclear periphery and never reaches the peak intensity seen in control cells (Fig. 6, A [bottom] and B; and Video 6). We conclude that PP2A-Tws promotes the timely recruitment of BAF to chromosomes during mitotic exit. Moreover, PP2A-Tws appears to be specifically required for the early phase of intense BAF recruitment to segregated chromosomes at the onset of NER. Further evidence that PP2A-Tws regulates the loading of BAF on reassembling nuclei comes from our observation that depletion of Endos, which selectively inhibits PP2A-Tws in early mitosis (Rangone et al., 2011), advances the recruitment of BAF (Fig. S4).

In *C. elegans*, the release of BAF from chromatin in mitosis is triggered by the phosphorylation of BAF by the VRK-1 kinase (Gorjánácz et al., 2007). Although *Drosophila* BAF is known to be required for normal cell cycle progression and NE organization in somatic cells, its regulation in mitosis has not been explored (Furukawa et al., 2003). However, in oogenesis, BAF is phosphorylated in prophase by the NHK-1 kinase, the orthologue of VRK-1 (Lancaster et al., 2007). As a result, chromosomes detach from the NE before it breaks down, forming a compact structure called the karyosome. Disruption of NHK-1–dependent phosphorylation of BAF results in persistent association between chromosomes and the NE, ensuing meiotic defects and female sterility (Lancaster et al., 2007). We hypothesized that the role of NHK-1 in phosphorylating BAF to trigger its release from chromatin in female meiosis may also be

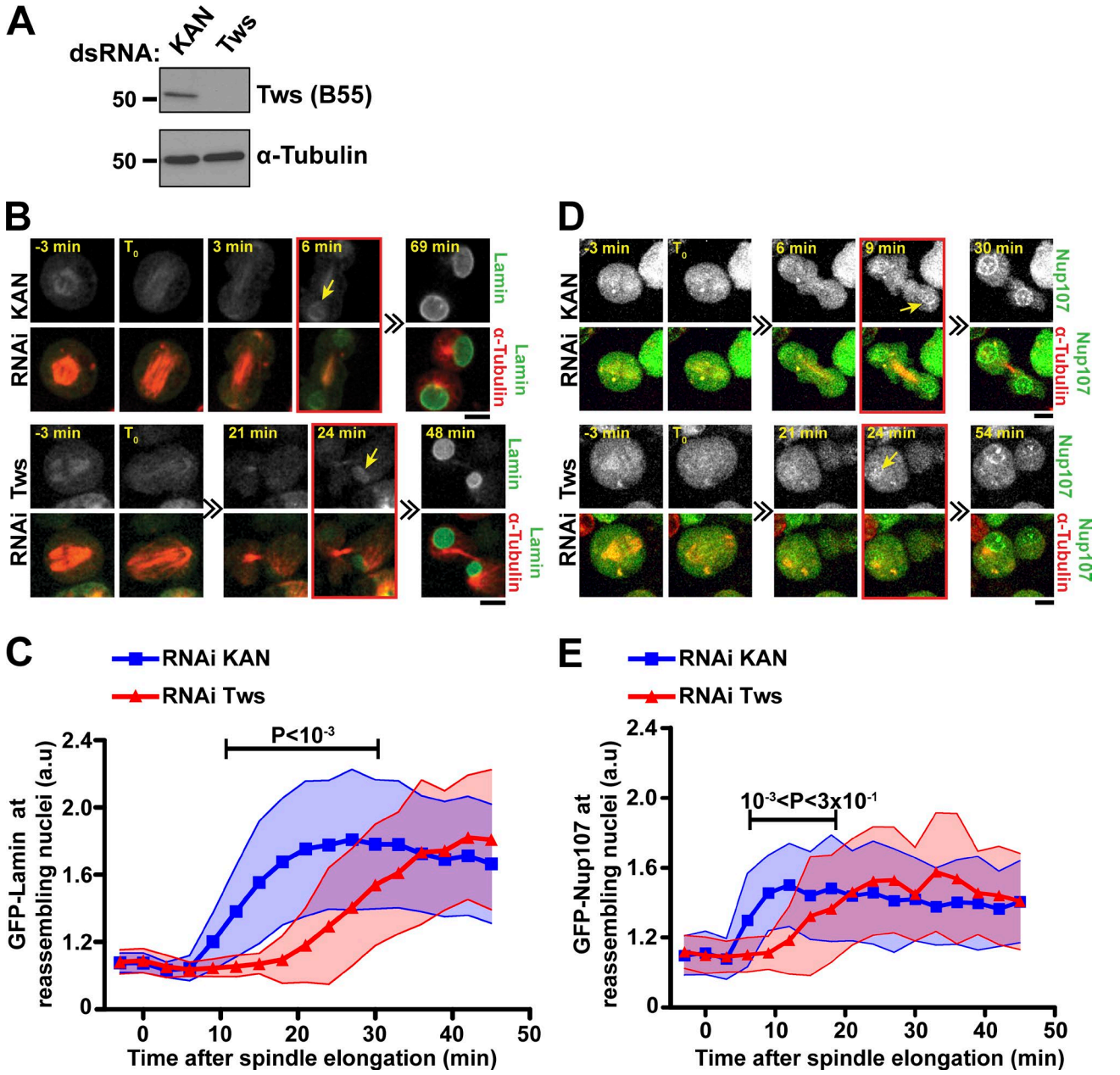

Figure 5. **PP2A-Tws is required for timely recruitment of Lamin and Nup107 to reassembling nuclei during mitotic exit. (A)** Western blots showing the RNAi depletion of Tws. **(B and D)** Live imaging of cells expressing GFP-Lamin (B) or GFP-Nup107 (D) and mCherry-Tubulin was performed after transfection with dsRNA against Tws or the bacterial KAN gene (nontarget control). Red frames and yellow arrow indicate the onset of recruitment of GFP-Lamin or Nup107-GFP to reassembling nuclei. Scale bars, 5 µm. **(C and E)** Quantification of GFP-Lamin or GFP-Nup107 recruitment on reassembling nuclei from the experiments in B and D. The fluorescence intensity in a fixed-size area at reassembling nuclei was quantified for each time point. Between 29 and 45 cells were quantified in each condition. Shaded areas indicate SD. P values are from a two-tailed *t* test.

important in mitosis in *Drosophila*. To test this, we mutated the three known NHK-1 phosphorylation sites in BAF (Lancaster et al., 2007) into alanine residues (BAF^{3A}; Fig. S5 A). GFP-BAF^{3A} remains on chromosomes in mitosis, unlike GFP-BAF^{WT}, suggesting that phosphorylation of BAF by NHK-1 is required for BAF dispersal in mitosis (Fig. 7, A and C, top; Videos 7 and 8; and Fig. S5 B). By contrast, the phosphomimetic GFP-BAF^{3D} was defective in its recruitment to chromosomes during mitotic exit compared with GFP-BAF^{WT} and its dynamics were similar to GFP-BAF^{WT} after depletion of Tws (Fig. S5 C; compare with Fig. 6 A). These results suggest that PP2A-Tws promotes the recruitment of BAF on reassembling nuclei by dephosphorylating NHK-1 sites on BAF.

We next tested if the Tws-dependent recruitment of BAF on chromosomes is sufficient for the recruitment of Lamin. In cells expressing both GFP-BAF^{WT} and RFP-Lamin, we found that depletion of Tws delays the recruitment of RFP-Lamin during NER, as expected (Fig. 7, A and B; and Video 9). In contrast, no delay of Lamin recruitment is observed in cells expressing GFP-BAF^{3A} depleted of Tws (Fig. 7, C and D; and Video 10).

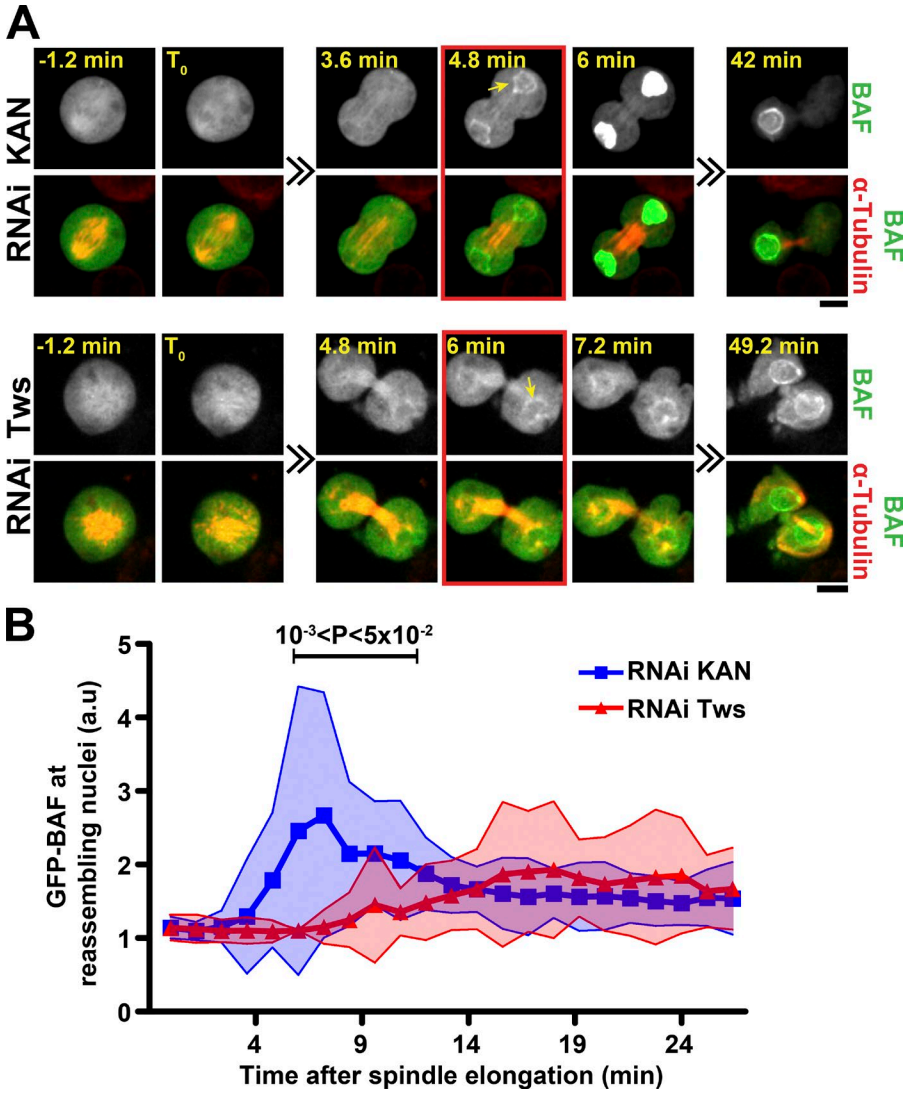

Figure 6. **PP2A-Tws is required for timely recruitment of BAF to reassembling nuclei during mitotic exit. (A)** Live imaging of cells expressing GFP-BAF and mCherry-Tubulin was performed after transfection with dsRNA against Tws or the bacterial KAN gene (nontarget control). Red frames and yellow arrow indicate the onset of recruitment of GFP-BAF. Scale bars, 5 µm. **(B)** Quantification of GFP-BAF recruitment on reassembling nuclei from the experiments in A. The fluorescence intensity in a fixed-size area at reassembling nuclei was quantified for each time point. For RNAi KAN and RNAi Tws, 26 and 25 cells were quantified, respectively. Shaded areas indicate the standard deviation. P values are from a two-tailed *t* test.

These results suggest that dephosphorylation of BAF by PP2A-Tws promotes Lamin recruitment during NER. However, the fact that GFP-BAF^{3A} does not retain Lamin on chromosomes throughout mitosis indicates that Lamin recruitment is not solely dependent on BAF dephosphorylation and is likely regulated by additional mechanisms. One of these mechanisms may be the direct dephosphorylation of Lamin by PP2A-Tws, as proposed above.

The above results suggest that the observed genetic interaction between *tws* and *lamin* in embryos may partly reflect a role of PP2A-Tws in the dephosphorylation of BAF at NHK-1 sites and that this dephosphorylation is required for Lamin recruitment to the reassembling NE. Thus, we hypothesized that weakening NHK-1 function in *lam*^{K2}*/+; tws*^{P}*/+* females might rescue their fertility. Interestingly, the introduction of a single copy of either one of two mutant alleles of *nhk-1* in *lam*^{K2}*/+; tws*^{P}*/+* females rescues the viability of the embryos they produce (Fig. 7 E). This result suggests that PP2A-Tws plays a critical role in antagonizing NHK-1 to promote NER after female meiosis and in syncytial mitoses.

Dephosphorylation of BAF promotes its association with Lamin

In vertebrates, BAF associates with Lamin via multiple LEM-domain proteins (Schellhaus et al., 2016). In human cells, these interactions are negatively regulated by the phosphorylation of BAF by NHK-1 (Margalit et al., 2007). Using coimmunoprecipitation, we confirmed that *Drosophila* BAF associates with Lamin. We used this assay to investigate how the BAF-Lamin association is regulated (Fig. 8 A). Treatment of cells with OA abolishes the association between GFP-BAF and Myc-Lamin, consistent with the idea that PP2A-Tws promotes the association between BAF and Lamin during NER (Fig. 8 A, lane 2 versus lane 1).

To test if the BAF-Lamin association is negatively regulated by NHK-1, we transfected cells with dsRNA against NHK-1 (or against KAN as a negative control). The efficiency of the dsRNA against NHK-1 was verified by monitoring the depletion of a PrA-tagged form of NHK-1 by Western blot (Fig. 8 B). We found that silencing NHK-1 tends to promote the BAF-Lamin association (Fig. 8 A, lane 4 versus lane 1) and even partially rescues this

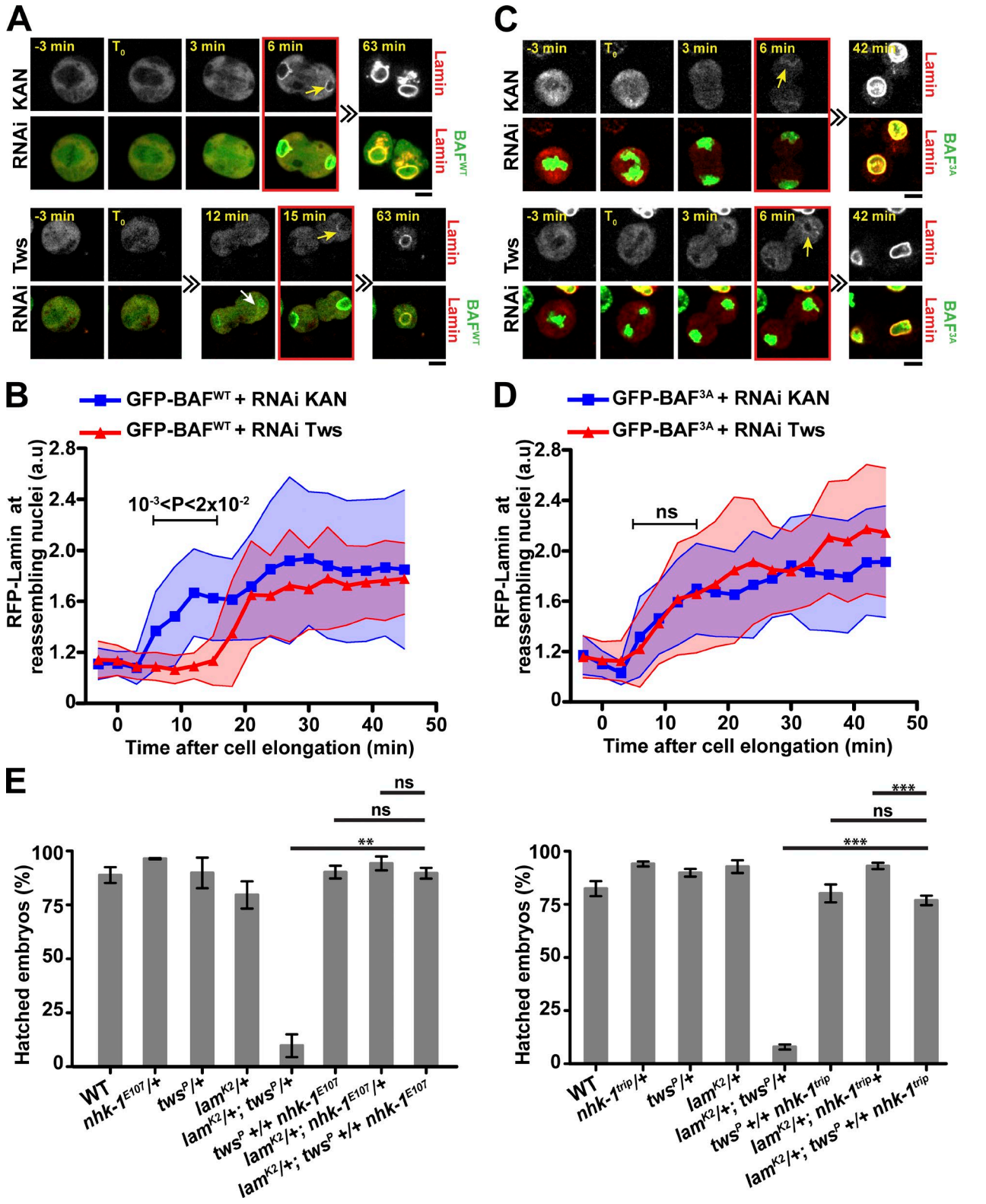

Figure 7. **The recruitments of BAF and Lamin to reassembling nuclei depend on BAF dephosphorylation. (A and C)** Live imaging in cells expressing RFP-Lamin and GFP-BAF^{WT} (A) or GFP-BAF^{3A} (C) was performed after transfection with dsRNA against Tws or the bacterial KAN gene (nontarget control). Red frames and yellow arrows indicate the onset of recruitment of RFP-Lamin to segregated chromosomes. The white arrow indicates BAF^{WT} recruitment. Scale bars, 5 µm. **(B and D)** Quantification of RFP-Lamin recruitment from the experiments in A and C. The fluorescence intensity in a fixed-size area at reassembling nuclei was quantified for each time point. Between 20 and 35 cells were quantified in each condition. Shaded areas indicate SD. **(E)** Introduction of one copy of mutant alleles of *nhk-1* in *lam^{K2}/+; tws^{P}/+* females rescues the development of embryos they produce. Percentages of hatching of embryos from females of the indicated genotypes were scored. Error bars represent SD. **, P = 0.0012; ***, P < 0.0001 two-tailed *t* test.

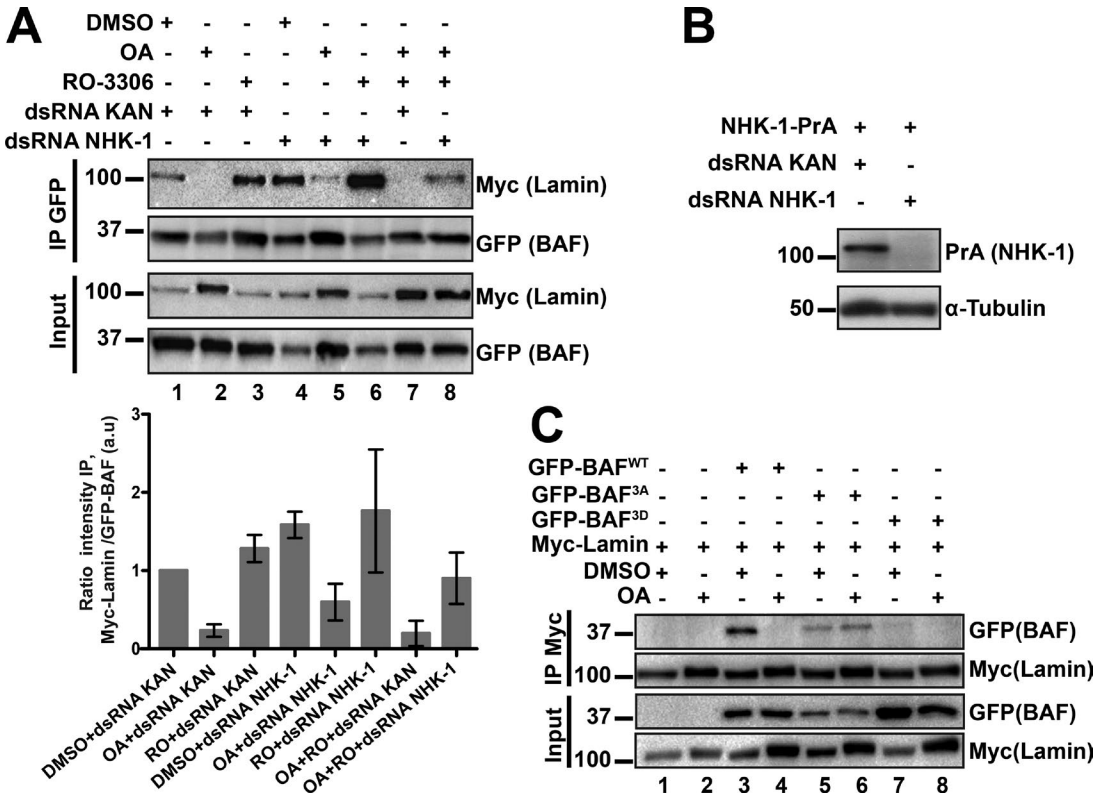

Figure 8. **The association between BAF and Lamin is regulated by mitotic kinases and phosphatases. (A)** Cells stably expressing GFP-BAF and Myc-Lamin were submitted to different treatments as indicated, followed by immunoprecipitation (IP) against GFP and Western blots. The ratios between coimmunoprecipitated Myc-Lamin and GFP-BAF, averaged between three experiments, is shown below. Error bars represent SEM. **(B)** The efficiency of the dsRNA against NHK-1 was verified by transfecting cells stably expressing NHK-1-PrA followed by Western blot. **(C)** Disruption of the BAF-Lamin association requires NHK-1 phosphorylation sites in BAF (experiment as in A).

association in OA-treated cells (lane 5 versus lane 2). Treating the cells with RO-3306, a CDK1 inhibitor that prevents mitotic entry, reinforces the association between BAF and Lamin, consistent with the idea that NHK-1 phosphorylates BAF in mitosis (Fig. 8 A). These results suggest that the BAF–Lamin association is negatively regulated by NHK-1 in mitosis.

To test if the disruption of the BAF–Lamin association by OA treatment depends on the NHK-1 phosphorylation sites on BAF, we performed copurifications using BAF^{3A} (Fig. 8 C). Unlike BAF^{WT}, which fails to associate with Lamin upon OA treatment (lane 4 versus lane 3), BAF^{3A} associates with Lamin even in the presence of OA (lane 6 vs lane 5). Conversely, BAF^{3D} fails to associate with Lamin even without OA treatment (lanes 7 and 8). These results suggest that NHK-1, by its known ability to phosphorylate BAF, disrupts the BAF-Lamin association and that OA-sensitive phosphatase activity, likely including PP2A-Tws, counteracts this phosphorylation to promote the BAF–Lamin association in addition to promoting the earlier recruitment of BAF to chromatin. We did not observe a decrease in the BAF–Lamin association upon Tws RNAi (data not shown). This result is expected because Tws RNAi delays Lamin recruitment by only 10–15 min (Fig. 7 B), and as *Drosophila* cells in culture are notoriously difficult to synchronize, the assay uses asynchronous cultures in which most cells are in interphase.

To explore when and where PP2A-Tws may regulate BAF in the cell, we used a proximal ligation assay (PLA), which monitors proximity between two proteins, as when they interact. A cell line stably expressing GFP-BAF and Myc-Tws was used, with primary antibodies against GFP and Myc. We detected abundant PLA foci between GFP-BAF and Myc-Tws (Fig. 9 A). The PLA signal is specific, as it is not detected in cells expressing only GFP-BAF or Myc-Tws or neither protein. Moreover, no PLA signal is detected in cells expressing both fusion proteins if either primary antibody is left out (data not shown). Interestingly, the number of PLA signal foci per cell is significantly higher in late mitosis and cytokinesis than in interphase and early mitosis. In addition, foci are mostly present in the cytoplasm (Fig. 9 A). These results are in agreement with a function of PP2A-Tws in the dephosphorylation of cytoplasmic BAF to promote its subsequent recruitment to the reassembling nuclei during mitotic exit.

We used an in vitro assay to test the dephosphorylation kinetics of a BAF peptide phosphorylated at Ser5 (BAF-pS5; Figs. S5 A). This site is equivalent to the known major NHK-1 site in human BAF, and its dephosphorylation was shown to promote BAF binding to DNA and LEM proteins at the NE (Nichols et al., 2006; Lancaster et al., 2007). As enzymes, we used PP2A obtained by immunoprecipitation of Flag-tagged regulatory subunits. We found that PP2A-Tws can dephosphorylate BAF-pS5 (Fig. 9 B). This reaction is slower than the dephosphorylation of well-documented PP2A-B55 sites in human PRC1 (PRC1-pT481 and PRC1-pT602; Cundell et al., 2013). This result is expected because PP2A-B55 enzymes are known to dephosphorylate pThr residues

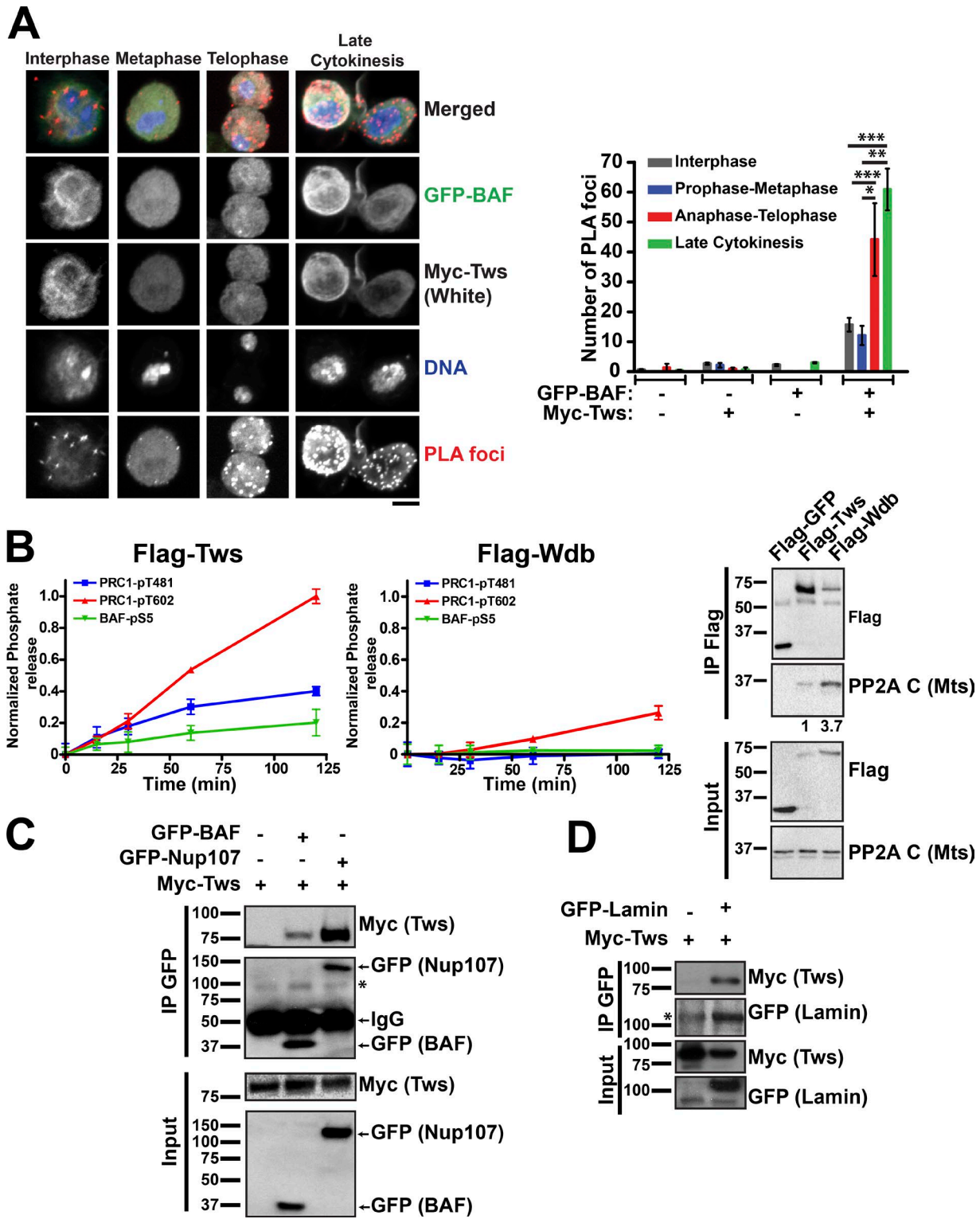

Figure 9. **Tws associates with BAF during mitotic exit and PP2A-Tws dephosphorylates BAF. (A)** PLA. Left: Cells transfected with Myc-Tws and GFP-BAF were submitted to PLA using antibodies against Myc and GFP (red foci). Immunofluorescence for Myc was done in parallel, and DNA was stained with DAPI. Right: Quantification of PLA foci per cell. Cells expressing only Myc-Tws or GFP-BAF were analyzed as controls. Error bars represent SEM. *, P = 0.0488; **, P = 0.0082; ***, P = 0.0002, two-tailed *t* test. Scale bar, 5 µm. **(B)** PP2A-Tws dephosphorylates a BAF peptide in vitro. Flag-Tws, Flag-Wdb, or Flag-GFP was immunoprecipitated and incubated with the indicated phosphopeptides for different times. Left: Phosphate release was measured as described in Materials and methods. Error bars represent SD. Right: Immunoprecipitation products were analyzed by Western blotting. The relative quantification of the Mts band intensities is shown below the blot. All results shown were obtained in the same (representative) experiment. Error bars represent SD from triplicates. **(C and D)** Cells transfected with the indicated proteins were submitted to coimmunopreciation against GFP followed by Western blot analysis. Asterisk indicates a background band in coimmunopreciation product (probably corresponding to a dimer of IgG heavy chain).

more rapidly than pSer residues in their substrates (Cundell et al., 2016; Hein et al., 2017). For comparison, we tested the ability of PP2A-Wdb/B56 to dephosphorylate the same sites, normalizing activities for the amount of the PP2A catalytic subunit (Mts) present in the reaction as quantified by Western blot. Consistent with results in human cells, PP2A-Wdb was capable of dephosphorylating PRC1-pT602 much better than PRC1-pT481 (Cundell et al., 2013). Very little activity of PP2A-Wdb was detected on BAF-pS5. These results confirm that Tws confers specificity to PP2A for its dephosphorylation of BAF at its major NHK-1 site.

Although our results strongly suggest that BAF is a target of PP2A-Tws, Lamin and Nup107 could also be its targets, as discussed above. We tested the ability of these proteins, tagged with GFP, to associate with Myc-tagged Tws, using coimmunopreciation. BAF, Lamin and Nup107 all associated specifically with Tws (Fig. 9, C and D). These results suggest that PP2A-Tws targets multiple proteins to promote NER.

Discussion

The molecular mechanisms mediating an orderly mitotic exit and return into interphase are much less understood than the mechanisms of mitotic entry. Moreover, while phosphatases are known to play crucial roles in promoting the mitosis to interphase transition, their specific contributions to the various events of this process remain largely unknown. Here, we have used the *Drosophila* system to search for and dissect the molecular events controlled by the PP2A-B55/Tws phosphatase in the cell cycle. Second-site noncomplementation screens have been used in various model organisms to identify functionally linked genes (Hawley and Gilliland, 2006). This work builds on the power of second-site noncomplementation maternal-effect screens in *Drosophila* to identify close collaboration between genes in cell cycle regulation (White-Cooper et al., 1996; Archambault et al., 2007; Wang et al., 2011).

Our genetic screen uncovered a strong link between PP2A-Tws and NER at the end of M phase. We found that simultaneously reducing the levels of Tws and Lamin in eggs using heterozygous mutations in mothers causes major defects in NER after meiosis II or after mitosis for embryos that initiated syncytial nuclear divisions. This result is striking considering that Lamin is not an essential protein in several cell types. Hypomorphic *lamin* mutants develop to adulthood, despite showing nuclear migration defects in photoreceptors and being female sterile (Patterson et al., 2004). In *lamin* null mutants, neuroblasts continue to proliferate in the absence of detectable Lamin (Osouda et al., 2005). In mice, the orthologous B-type lamins are dispensable for cell viability and proliferation, at least in keratinocytes; however, B-type lamins are essential in neurons (Yang et al., 2011). In general, B-type lamins may play a crucial role in structuring nuclei and withstanding force in cells where nuclear migration/positioning is essential. Such cell types include *Drosophila* eggs, where pronuclei must converge before fusing, and syncytial embryos, where nuclei migrate toward the cortex.

Using cells in culture, we found that PP2A-Tws promotes the recruitment of several NE components after mitosis, namely BAF, Lamin, and Nup107. In *Drosophila* oogenesis, BAF phosphorylation by NHK-1 promotes the detachment of chromatin from the germinal vesicle during karyosome formation (Lancaster et al., 2007). In this work, we found that BAF requires NHK-1 phosphorylation sites to dissociate from chromatin during NEB, as in *C. elegans* (Gorjánácz et al., 2007; Asencio et al., 2012). Our genetic, biochemical and imaging results suggest that phosphorylation of BAF by NHK-1 is reversed by PP2A-Tws to promote its recruitment on chromatin at the onset of NER (Fig. 10). This is consistent with results in *C. elegans* that showed a role for PP2A in this process, although the relevant phosphorylation sites in BAF were not investigated and the PP2A adaptor subunit involved was unclear (Asencio et al., 2012). Recent work shows that BAF plays a crucial role in holding chromosomes together just after anaphase to promote the assembly of the NE around a single nucleus (Samwer et al., 2017). Our findings suggest that PP2A-Tws dephosphorylates BAF to promote this function. Our results also suggest that regulation of BAF phosphorylation by NHK-1 and PP2A-Tws regulates its ability to form complexes with Lamin. In vertebrates, BAF is known to interact with lamins via LEM domain proteins at the NE (Schellhaus et al., 2016). Human BAF phosphorylation by VRK1/NHK-1 decreases its ability to interact with a LEM domain (Nichols et al., 2006). LEM-domain proteins have also been shown to be phosphorylated to negatively regulate their ability to interact with BAF in *X. laevis* extracts (Hirano et al., 2005, 2009). Thus, PP2A-B55 could dephosphorylate LEM proteins to further promote their association with BAF during NER, and this possibility should be investigated.

By inducing the recruitment of BAF on reassembling nuclei, PP2A-Tws likely promotes the recruitment of multiple downstream NE components. Nevertheless, PP2A-Tws likely has other targets in NER, possibly including Lamin and Nup107 (Fig. 10). Both proteins contain multiple CDK phosphorylation motifs, and PP2A-B55 enzymes have been shown to dephosphorylate many such sites efficiently (Mayer-Jaekel et al., 1994; Castilho et al., 2009; Mochida et al., 2009). Moreover, we observed that Lamin and Nup107 both associate with Tws. We found that mutation of all CDK consensus sites in Lamin prevents lamina disassembly in mitosis and, although the attempted phospho-mimetic mutation of all sites did not disrupt lamina assembly in live cells, it increases Lamin solubility in cell lysates. The CDK sites on Lamin are grouped in two clusters flanking the coiled region, and some of these sites have already been shown to negatively regulate homotypic interactions of Lamin (Fig. 4 A; Machowska et al., 2015). We have not explored the effect of mutating CDK sites in Nup107. However, Nup107 is rapidly dephosphorylated at multiple sites during mitotic exit in human cells (McCloy et al., 2015) and dephosphorylation of at least one CDK site in Nup107 was shown to depend on PP2A-B55 (Cundell et al., 2016). However, although PP2A-B55 is capable of dephosphorylating several CDK sites, many of these sites are probably regulated mainly by another phosphatase in vivo. Moreover, numerous examples of PP2A-B55–dependent, non-CDK sites were recently identified (Cundell et al., 2016). This is further exemplified here by the dephosphorylation of BAF by PP2A-Tws at a NHK-1 site, which cannot be a CDK site, as it lacks the proline residue in position +1. Nevertheless, with its positively charged amino acid residues in positions +2 to +4 (Fig. S5), this site resembles the recently

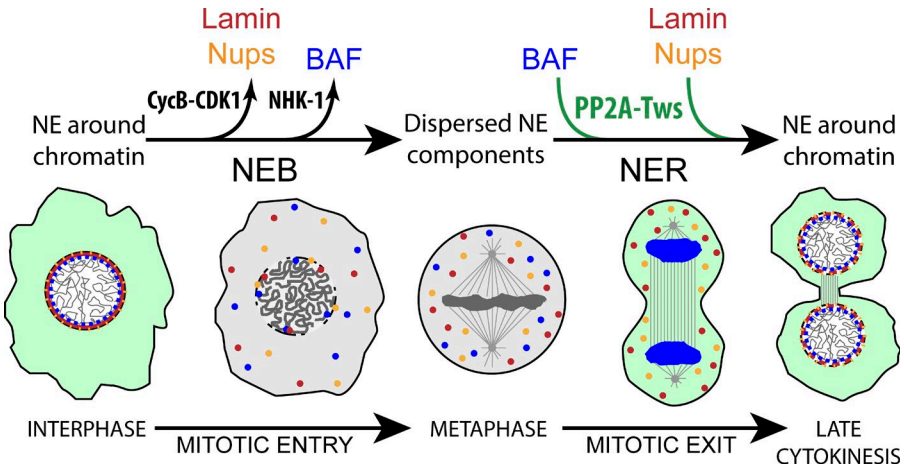

Figure 10. **Model for the role of PP2A-Tws in promoting NER after mitosis.** As the cell enters mitosis, Cyclin B-CDK1 phosphorylates Lamin (red) and probably other proteins, including Nup107 (Nups are in yellow), to induce NEB. NHK-1 phosphorylates BAF (blue), inducing its dissociation from chromatin. As the cell exits mitosis, PP2A-Tws dephosphorylates BAF, inducing its rapid recruitment to condensed chromatin in late anaphase (green indicates PP2A-Tws active). Lamin and Nup107 are likely also dephosphorylated by PP2A-Tws to promote their assembly in NEs. When the NE is reformed, BAF becomes restricted to the inner periphery of the nucleus.

defined PP2A-B55 consensus motif (Cundell et al., 2016) and a consensus motif for sites lacking a Pro residue at position +1 but that are rapidly dephosphorylated during mitotic exit (McCloy et al., 2015).

Overall, PP2A-B55 appears to target multiple proteins, dephosphorylating them at various sites that depend on multiple kinases, to promote NER cooperatively. A recent phosphoproteomic study found that several proteins of the NE are particularly prone to rapid dephosphorylation during mitotic exit, in a process that likely involves other phosphatases (McCloy et al., 2015). Much work remains to be done to fully dissect the mechanisms at play. The fact that NER is only delayed and not completely prevented when PP2A-Tws is silenced in cell culture could be due to an incomplete inactivation of PP2A-Tws inherent to the RNAi approach. Alternatively, other phosphatases may partially compensate for the loss of PP2A-Tws activity. Protein phosphatase 4 (PP4) may function in this way as it has been shown to dephosphorylate BAF in human cells (Zhuang et al., 2014). In addition, protein phosphatase 1 enzymes likely contribute to NER in *Drosophila*, as they promote this process through multiple mechanisms in vertebrates, including the dephosphorylation of Lamin B (Thompson et al., 1997; de Castro et al., 2016).

Our screen results point at other functions of PP2A-Tws in the completion of M phase that remain to be explored, although some of the genetic interactions identified could reflect roles of PP2A-Tws unrelated to mitotic regulation. Our preliminary, unpublished results suggest that the genetic interaction between *tws* and *CycB3* reflects their collaboration in the completion of meiosis (Fig. S1 A). Interestingly, we uncovered genetic interactions between *tws* and genes that encode nucleocytoplasmic transport factors. Mutations in the gene for Cse1/CAS, which transports importin α back to the cytoplasm to promote its function in nuclear import, enhances *tws*-dependent embryonic lethality (Fig. S1 A; Tekotte et al., 2002). Conversely, mutations in *embargoed* (*emb*), which encodes the nuclear export factor Crm1, rescues *tws*-dependent embryonic lethality (Fig. S1 B; Collier et al., 2000). These results suggest that active nuclear import plays an important role in NER or other aspects of the establishment of interphase nuclei after mitosis and/or meiosis, presumably by promoting the nuclear localization of crucial enzymes or structural factors. Defining these factors and the regulation of their nucleocytoplasmic transport during mitotic exit should be the topic of future investigations.

In this work, we have used a genetic strategy to search for the roles of PP2A-Tws in the cell cycle in vivo. We found that PP2A-Tws promotes NER, and we have begun to dissect the mechanisms at play. This study opens the door to the use of *Drosophila* to gain a better mechanistic understanding of NER at the molecular level. Moreover, it will be a powerful system to further dissect the functions of PP2A-Tws and other phosphatases in the coordination of mitotic exit.

Materials and methods

Plasmids and mutagenesis

Plasmids were generated using the Gateway recombination system (Invitrogen). The cDNA of each gene was cloned in a pDONOR221 entry vector before being recombined into destination vectors containing copper-inducible (pMT) or constitutive (pAC5) promoters. The following plasmids were generated: pAC5-GFP-Lamin^{WT}, pAC5-Myc-Lamin^{WT}, pAC5-Myc-Lamin^{7A}, pAC5-Myc-Lamin^{7D}, pMT-RFP-Lamin^{WT}, pMT-RFP-Lamin^{7A}, pMT-RFP-Lamin^{7D}, pAC5-mCherry-Tubulin, pMT-GFP-Nup107, pMT-GFP-BAF^{WT}, pMT-GFP-BAF^{3A}, pMT-GFP-BAF^{3D}, pAC5-Myc-Tws, pAC5-GFP-Tws, pAC5-Flag-Tws, pAC5-Flag-Wdb, pAC5-Flag-GFP, and pAC5-NHK-1-PrA. Amino acid substitution mutants were generated using QuikChange Lightning Site-Directed Mutagenesis Kit (Agilent) as described by the manufacturer. cDNAs for plasmids expressing Lamin mutants were generated by BioBasic.

Fly culture, genetic screen, and fertility tests

Fly culture was done according to standard procedures. For the genetic screen, a collection of 417 lines containing most Drosdel deficiencies and a few additional ones (obtained from Martin Lefrançois and Marc Therrien, Université de Montréal, Montréal, Canada) covering most of chromosomes II and III was used (see Table S1 for the complete list). Each line was crossed to the *y w; tws^{P}/TM6B* or *mts$^{XE-2258}$/CyO* lines. Flies heterozygous for both the deletion and the *tws^{P}* or *mts$^{XE-2258}$* mutation were selected based on the absence of balancer chromosomes, and their fertility was tested (see below). Table S3 provides a list of all mutant

alleles used in this study, their molecular lesion, and their origin. Mutant fly lines were obtained from the Bloomington *Drosophila* Stock Center (Bloomington, IN), Aldelaide Carpenter and David Glover (University of Cambridge, Cambridge, England), Hiroyuki Ohkura (Wellcome Trust Centre for Cell Biology, Edinburgh, Scotland), or Marc Therrien (Université de Montréal, Montréal, QC, Canada). Flies expressing GFP-Polo were obtained from Claudio Sunkel (Instituto de Biologia Molecular e Celular, Porto, Portugal).

For fertility tests shown in Figs. 4 E, 7 E (left), and S1 B and Table S2, three to five virgin females 1 to 4 d old were crossed with three to five Oregon R males per tube and kept at 25°C for 1 d. Flies were then transferred to tubes containing grape juice agar with yeast paste. After 1 d, flies were transferred again to new tubes. 24 h later, the percentage of hatched embryos was counted. Approximately 100 embryos were counted each time, and this scoring was repeated at least three times. For experiments shown in Figs. 2 A, 7 E (right), S1 A ,and S3, the fertility of five to 10 single virgin females crossed with three to five Oregon R males was scored. For the genetic screen (Fig. 1 D and Table S1), the fertility of a group of three to five females (not necessarily virgins) crossed to three to five Oregon R males was scored on three consecutive days, and numbers were pooled.

Embryo and egg immunostaining

For immunofluorescence shown in Figs. 2 C, S2, and S3, females were kept to lay embryos on grape juice agar for 2 h at 25°C. Embryos were immediately dechorionated and fixed as described previously (Archambault et al., 2007). The following primary antibodies were used for staining: anti-Lamin Dm0 ADL84.12 from mouse (1:100; Developmental Studies Hybridoma Bank), anti–α-Tubulin YL1/2 from rat (1:50, #6160; Abcam), and anti–γ-Tubulin GTU-88 from mouse (1:50, #T5326; Sigma). After an overnight incubation of primary antibodies at 4°C, embryos were incubated with secondary antibodies coupled to Alexa Fluor 488 (1:200; Invitrogen) or Cy3 (1:200; Jackson) for 2 h at room temperature. DNA was marked with DAPI. Embryos were mounted using Vectashield (Vector Laboratories). Images were generated using an LSM 700 confocal microscope (Zeiss) with a 63× oil objective and treated using Photoshop.

For examining meiosis (Fig. 3), females were kept to lay eggs on an agar plate for 20 min, after which eggs were dechorionated and washed in a solution of 0.7% NaCl and 0.05% Triton X-100. Eggs were then fixed in a 1:1 heptane/methanol solution before being washed in 100% methanol; rehydrated sequentially in 90%, 70%, and 50% methanol; and washed in PBS + 0.2% Tween. Eggs were then incubated with 1:100 anti–Lamin ADL 67.10 from mouse (Developmental Studies Hybridoma Bank), 1:2,000 rat anti–α-Tubulin YL1/2 (Sigma) and Oligreen (Invitrogen). Secondary Alexa-conjugated antibodies were used (1:1,000). Eggs were then mounted using 1,2,3,4-Tetrahydronaphthalene (Sigma). Images were taken on an Olympus FV1000 scanning confocal microscope with a 60× water objective lens.

Drosophila cell culture and drug treatments

D-Mel2 cells were cultured in Express Five medium (Invitrogen) supplemented with glutamine, penicillin, and streptomycin. Stable cell lines were generated in a selection medium containing 10 µg/ml blasticidin. Expression of transgenes under a copper-inducible promoter was induced by adding $CuSO_4$ (300 µM) to the media for at least 8 h. For phosphatase inhibition, cells were treated with 100 nM OA (Bioshop) for 30 min before being lysed for immunoprecipitation. For CDK1 inhibition, cells were treated with 10 µM RO-3306 (Tocris Bioscience) for 1 h and 30 min before being lysed.

Transient transfections

D-Mel2 cells of 70% to 80% confluence in six-well plates or 25-cm^2 flasks were transfected with 2.5 µg or 5 µg plasmids, respectively, using the X-tremeGene HP DNA transfection reagent (Roche) as instructed by the manufacturer. Cells were cultured between 24 and 72 h at 25°C before being assayed. For RNAi, cells of 60–70% confluence were plated in six-well plates and transfected with 25 µg dsRNA for Tws, NHK-1, or Endos, along with the Transfast reagent (Promega). dsRNA against the bacterial resistance gene KAN was used as a nontarget control. Cells were incubated at 25°C for 72–96 h before being analyzed.

Time-lapse microscopy

Time-lapse fluorescence imaging of cultured cells and embryos was performed on a spinning-disk confocal system (CSU-X1 5000; Yokogawa) mounted on a fluorescence microscope (Axio Observer.Z1; Zeiss) using a 63× oil objective an Axiocam 506 mono camera (Zeiss).

PLA

D-Mel2 cells stably expressing GFP-Tws and Myc-BAF^{WT} were fixed using 4% formaldehyde (Sigma), after which cells were blocked then incubated with anti-GFP from rabbit (1:200; Invitrogen) and anti-Myc 9E10 from mouse (1:200; Santa Cruz Biotechnology, Inc.) for 1 h at room temperature. PLA was performed using the Duolink starter kits (Sigma) as described by the manufacturer. The Duolink anti-rabbit plus and anti-mouse minus probes were used. During the amplification step, cells were incubated with secondary antibodies coupled to Alexa Fluor 488 from rabbit (1:200; Invitrogen), Cy3 from mouse (1:200; Jackson), and Alexa Fluor 566 from mouse for 2 h at room temperature. DAPI was used to stain DNA. Images were taken using a LSM 700 confocal microscopy and treated using Photoshop.

Immunoprecipitation and Western blotting

For each sample, between 4 and 20 million cells transfected as above were harvested and washed in PBS containing protease inhibitors (1 mM PMSF, 10 µg/ml aprotinin, and 10 µg/ml leupeptin). Cells were lysed in 75 mM K-Hepes, pH 7.5, 150 mM NaCl, 1 mM DTT, 2 mM $MgCl_2$, 2 mM EGTA, and 1% Triton X-100, with protease inhibitors as above. Lysates were centrifuged at 14,600 rpm for 10 min at 4°C. Clarified lysates were incubated with anti-GFP from rabbit (Invitrogen) on a wheel for 1 h at 4°C and then incubated with 15 to 20 µl protein A–conjugated Dynabeads suspension (Life Technologies) for another 45 min at 4°C. Beads were washed in 1 ml lysis buffer 4 × 5 min and eluted directly in Laemmli sample buffer for SDS-PAGE. Antibodies used in Western blotting were anti-GFP from rabbit (Invitrogen), anti-Myc 9E10

from mouse (Santa Cruz Biotechnology, Inc.), anti-Lamin Dm0 (DSHB Hybridoma Product ADL84.12), anti–α-Tubulin DM1A from mouse (Sigma), anti-Tws from rabbit (Thermo Fisher Scientific), anti-H3 from rabbit (NEB), anti-Endos from rabbit (custom made by Thermo Fisher Scientific), anti-Flag M2 from mouse (Sigma), peroxidase-conjugated purified rabbit IgG (Jackson), peroxidase-conjugated AffiniPure Goat anti–mouse IgG (Jackson), and peroxidase-conjugated AffiniPure Goat anti–rabbit IgG (Jackson). For analyzing protein levels of mutant embryos of Fig. 2, embryos from Oregon R and single- and double-mutant females were collected as described above and washed with PBS solution containing protease inhibitors before being crushed and clarified by centrifugation at 14,600 rpm for 10 min at 4°C. Before SDS-PAGE, protein levels in supernatants were quantified using the Bradford protein assay kit (Bio-Rad). The same masses of total proteins were loaded for all samples, and proteins were analyzed by immunoblotting.

Phosphatase assay

Approximately 200 million D-mel2 cells stably expressing either Flag-Tws, Flag-Wdb, or Flag-GFP were collected and centrifuged at 1,500 rpm for 5 min at 4°C. Pellets were suspended in TBS containing protease inhibitors (1 mM PMSF, 10 µg/ml aprotinin, and 10 µg/ml leupeptin). Cells were lysed in buffer containing 20 mM Tris-HCl, pH 7.5, 150 mM NaCl, 2 mM EGTA, 0.5% NP-40, 1 mM DTT, and protease inhibitors (as above) and incubated on a wheel for 15 min at 4°C before being centrifuged at 4,600 rpm for 15 min at 4°C. Supernatants were incubated with anti-Flag antibody for 75 min on a wheel at 4°C and with protein G–conjugated Dynabeads (Life Technologies) for an additional 45 min. Beads were washed 4 × 5 min with lysis buffer before being used as sources of enzymes for the phosphatase assay. The following peptides were used as substrates: BAF-pS5, MSGTpSQKHRNFVAEPMGNK; PRC1-pT481, SKRRGLAPNpTPG KARKLNTTT; PRC1-pT602, LSKASKSDATSGILNSpTNIQS (all synthesized by Biobasic). The 2× reaction solutions contained 400 µM peptides, 20 mM Tris, pH 7.5, 5 mM $MgCl_2$, 1 mM EGTA, 20 mM β-mercaptoethanol, and 1.45 mg/ml of BSA. For the phosphatase reactions, equal volumes of 2× reaction solution and washed bead suspensions were combined and incubated at room temperature in 96-well plates. Reactions were stopped by the addition of 90 mM $HClO_4$. Phosphate release was revealed by the addition of one volume of 1 M malachite green solution. The absorbance was then measured at a wavelength of 620 nm using a plate reader (Tecan Infinite 200 PRO). For results presented in Fig. 9 B, the colorimetric measurements obtained with Flag-GFP for each time points were subtracted from the measurements obtained with Flag-Tws and Flag-Wdb. Values for T_0 were also subtracted from both series. All values were normalized by fixing the highest value obtained to 1 (the activity associated with Flag-Tws on PRC1-pT602 peptide after 2 h). In addition, activities were normalized for the amount of PP2A catalytic subunit (Mts) present in the reactions by dividing the activities associated with Flag-Wdb by the ratio of the Mts band intensities from the Flag-Wdb immunoprecipitated/Flag-Tws immunoprecipitated complexes.

Online supplemental material

Fig. S1 shows the genetic interactions of PP2A-Tws identified. Fig. S2 shows that embryos from females heterozygous for lam^{K2} or tws^{P} alleles alone show only minor developmental defects. Fig. S3 shows that a collaboration between PP2A-Tws and Nup107 is required for syncytial embryonic development. Fig. S4 shows that depletion of Endos advances the recruitment of BAF on reassembling nuclei after mitosis. Fig. S5 shows that phosphorylation of BAF at NHK-1 sites controls its localization in mitosis. Table S1 lists complete results from the genetic deletion screen. Table S2 shows a screen for genetic interactions between *lamin* and genes encoding various phosphatase subunits. Table S3 lists the mutant alleles used in this study, their source, and their molecular lesion. Video 1 shows normal development in an embryo expressing GFP-Polo from a WT mother. Video 2 shows abnormal development in an embryo expressing GFP-Polo from a $lam^{K2}/+; tws^{P}/+$ mother. Video 3 shows division of a cell stably expressing RFP-$Lamin^{WT}$ that becomes dispersed in mitosis and is reassembled during mitotic exit. Video 4 shows division of a cell stably expressing RFP-$Lamin^{7A}$ that is not dispersed in mitosis. Video 5 shows division of a cell stably expressing GFP-BAF and mCherry-Tubulin transfected with control dsRNA against KAN. Video 6 shows division of a cell stably expressing GFP-BAF and mCherry-Tubulin transfected with dsRNA against Tws. Video 7 shows division of a cell stably expressing GFP-BAF and RFP-Lamin transfected with control dsRNA against KAN. Video 8 shows division of a cell stably expressing GFP-BAF^{3A} and RFP-Lamin transfected with control dsRNA against KAN. Video 9 shows division of a cell stably expressing GFP-BAF and RFP-Lamin transfected with dsRNA against Tws. Video 10 shows division of a cell stably expressing GFP-BAF^{3A} and RFP-Lamin transfected with dsRNA against Tws.

Acknowledgments

We thank Martin Lefrançois, Marc Therrien, David Glover, Adelaide Carpenter, Hiro Ohkura, Claudio Sunkel, and the Bloomington *Drosophila* Stock Center for fly lines. We thank members of the V. Archambault laboratory for comments and discussions.

This work was supported by the Canadian Institutes of Health Research (grant MOP-133558 to V. Archambault) and the Natural Sciences and Engineering Research Council of Canada (grants 402217-2011 RGPIN to V. Archambault and RGPIN-2017-05839 to A. Swan). H. Mehsen, V. Boudreau, D. Garrido, M. Larouche, and V. Archambault hold or held a scholarship from the Fonds de Recherche du Québec – Santé. The Institute for Research in Immunology and Cancer is supported in part by the Canada Foundation for Innovation and the Fonds de Fecherche du Québec – Santé.

The authors declare no competing financial interests.

Author contributions: V. Archambault, H. Mehsen, and V. Boudreau designed the project. H. Mehsen, V. Boudreau, D. Garrido, M. Bourouh, M. Larouche, and A. Swan conducted the experiments. V. Archambault, A. Swan, and P. Maddox supervised the work. V. Archambault, H. Mehsen, A. Swan, V. Boudreau, and M. Bourouh wrote the paper.

Submitted: 3 April 2018
Revised: 17 August 2018
Accepted: 5 September 2018

References

Afonso, O., I. Matos, A.J. Pereira, P. Aguiar, M.A. Lampson, and H. Maiato. 2014. Feedback control of chromosome separation by a midzone Aurora B gradient. *Science.* 345:332–336. https://doi.org/10.1126/science.1251121

Archambault, V., X. Zhao, H. White-Cooper, A.T. Carpenter, and D.M. Glover. 2007. Mutations in Drosophila Greatwall/Scant reveal its roles in mitosis and meiosis and interdependence with Polo kinase. *PLoS Genet.* 3:e200. https://doi.org/10.1371/journal.pgen.0030200

Archambault, V., G. Lépine, and D. Kachaner. 2015. Understanding the Polo Kinase machine. *Oncogene.* 34:4799–4807. https://doi.org/10.1038/onc.2014.451

Asencio, C., I.F. Davidson, R. Santarella-Mellwig, T.B. Ly-Hartig, M. Mall, M.R. Wallenfang, I.W. Mattaj, and M. Gorjánácz. 2012. Coordination of kinase and phosphatase activities by Lem4 enables nuclear envelope reassembly during mitosis. *Cell.* 150:122–135. https://doi.org/10.1016/j.cell.2012.04.043

Carmena, M., S. Ruchaud, and W.C. Earnshaw. 2009. Making the Auroras glow: regulation of Aurora A and B kinase function by interacting proteins. *Curr. Opin. Cell Biol.* 21:796–805. https://doi.org/10.1016/j.ceb.2009.09.008

Castilho, P.V., B.C. Williams, S. Mochida, Y. Zhao, and M.L. Goldberg. 2009. The M phase kinase Greatwall (Gwl) promotes inactivation of PP2A/B55delta, a phosphatase directed against CDK phosphosites. *Mol. Biol. Cell.* 20:4777–4789. https://doi.org/10.1091/mbc.e09-07-0643

Clever, M., T. Funakoshi, Y. Mimura, M. Takagi, and N. Imamoto. 2012. The nucleoporin ELYS/Mel28 regulates nuclear envelope subdomain formation in HeLa cells. *Nucleus.* 3:187–199. https://doi.org/10.4161/nucl.19595

Collier, S., H.Y. Chan, T. Toda, C. McKimmie, G. Johnson, P.N. Adler, C. O'Kane, and M. Ashburner. 2000. The Drosophila embargoed gene is required for larval progression and encodes the functional homolog of schizosaccharomyces Crm1. *Genetics.* 155:1799–1807.

Cundell, M.J., R.N. Bastos, T. Zhang, J. Holder, U. Gruneberg, B. Novak, and F.A. Barr. 2013. The BEG (PP2A-B55/ENSA/Greatwall) pathway ensures cytokinesis follows chromosome separation. *Mol. Cell.* 52:393–405. https://doi.org/10.1016/j.molcel.2013.09.005

Cundell, M.J., L.H. Hutter, R. Nunes Bastos, E. Poser, J. Holder, S. Mohammed, B. Novak, and F.A. Barr. 2016. A PP2A-B55 recognition signal controls substrate dephosphorylation kinetics during mitotic exit. *J. Cell Biol.* 214:539–554. https://doi.org/10.1083/jcb.201606033

de Castro, I.J., E. Gokhan, and P. Vagnarelli. 2016. Resetting a functional G1 nucleus after mitosis. *Chromosoma.* 125:607–619. https://doi.org/10.1007/s00412-015-0561-6

Furukawa, K., S. Sugiyama, S. Osouda, H. Goto, M. Inagaki, T. Horigome, S. Omata, M. McConnell, P.A. Fisher, and Y. Nishida. 2003. Barrier-to-autointegration factor plays crucial roles in cell cycle progression and nuclear organization in Drosophila. *J. Cell Sci.* 116:3811–3823. https://doi.org/10.1242/jcs.00682

Gharbi-Ayachi, A., J.C. Labbé, A. Burgess, S. Vigneron, J.M. Strub, E. Brioudes, A. Van-Dorsselaer, A. Castro, and T. Lorca. 2010. The substrate of Greatwall kinase, Arpp19, controls mitosis by inhibiting protein phosphatase 2A. *Science.* 330:1673–1677. https://doi.org/10.1126/science.1197048

Glavy, J.S., A.N. Krutchinsky, I.M. Cristea, I.C. Berke, T. Boehmer, G. Blobel, and B.T. Chait. 2007. Cell-cycle-dependent phosphorylation of the nuclear pore Nup107-160 subcomplex. *Proc. Natl. Acad. Sci. USA.* 104:3811–3816. https://doi.org/10.1073/pnas.0700058104

Glover, D.M. 1989. Mitosis in Drosophila. *J. Cell Sci.* 92:137–146.

Gorjánácz, M., E.P. Klerkx, V. Galy, R. Santarella, C. López-Iglesias, P. Askjaer, and I.W. Mattaj. 2007. Caenorhabditis elegans BAF-1 and its kinase VRK-1 participate directly in post-mitotic nuclear envelope assembly. *EMBO J.* 26:132–143. https://doi.org/10.1038/sj.emboj.7601470

Haraguchi, T., T. Koujin, M. Segura-Totten, K.K. Lee, Y. Matsuoka, Y. Yoneda, K.L. Wilson, and Y. Hiraoka. 2001. BAF is required for emerin assembly into the reforming nuclear envelope. *J. Cell Sci.* 114:4575–4585.

Haraguchi, T., T. Kojidani, T. Koujin, T. Shimi, H. Osakada, C. Mori, A. Yamamoto, and Y. Hiraoka. 2008. Live cell imaging and electron microscopy reveal dynamic processes of BAF-directed nuclear envelope assembly. *J. Cell Sci.* 121:2540–2554. https://doi.org/10.1242/jcs.033597

Hawley, R.S., and W.D. Gilliland. 2006. Sometimes the result is not the answer: the truths and the lies that come from using the complementation test. *Genetics.* 174:5–15. https://doi.org/10.1534/genetics.106.064550

Heald, R., and F. McKeon. 1990. Mutations of phosphorylation sites in lamin A that prevent nuclear lamina disassembly in mitosis. *Cell.* 61:579–589. https://doi.org/10.1016/0092-8674(90)90470-Y

Heim, A., A. Konietzny, and T.U. Mayer. 2015. Protein phosphatase 1 is essential for Greatwall inactivation at mitotic exit. *EMBO Rep.* 16:1501–1510. https://doi.org/10.15252/embr.201540876

Hein, J.B., E.P.T. Hertz, D.H. Garvanska, T. Kruse, and J. Nilsson. 2017. Distinct kinetics of serine and threonine dephosphorylation are essential for mitosis. *Nat. Cell Biol.* 19:1433–1440. https://doi.org/10.1038/ncb3634

Hirano, Y., M. Segawa, F.S. Ouchi, Y. Yamakawa, K. Furukawa, K. Takeyasu, and T. Horigome. 2005. Dissociation of emerin from barrier-to-autointegration factor is regulated through mitotic phosphorylation of emerin in a xenopus egg cell-free system. *J. Biol. Chem.* 280:39925–39933. https://doi.org/10.1074/jbc.M503214200

Hirano, Y., Y. Iwase, K. Ishii, M. Kumeta, T. Horigome, and K. Takeyasu. 2009. Cell cycle-dependent phosphorylation of MAN1. *Biochemistry.* 48:1636–1643. https://doi.org/10.1021/bi802060v

LaJoie, D., and K.S. Ullman. 2017. Coordinated events of nuclear assembly. *Curr. Opin. Cell Biol.* 46:39–45. https://doi.org/10.1016/j.ceb.2016.12.008

Lancaster, O.M., C.F. Cullen, and H. Ohkura. 2007. NHK-1 phosphorylates BAF to allow karyosome formation in the Drosophila oocyte nucleus. *J. Cell Biol.* 179:817–824. https://doi.org/10.1083/jcb.200706067

Lindqvist, A., V. Rodríguez-Bravo, and R.H. Medema. 2009. The decision to enter mitosis: feedback and redundancy in the mitotic entry network. *J. Cell Biol.* 185:193–202. https://doi.org/10.1083/jcb.200812045

Lyakhovetsky, R., and Y. Gruenbaum. 2014. Studying lamins in invertebrate models. *Adv. Exp. Med. Biol.* 773:245–262. https://doi.org/10.1007/978-1-4899-8032-8_11

Ma, S., S. Vigneron, P. Robert, J.M. Strub, S. Cianferani, A. Castro, and T. Lorca. 2016. Greatwall dephosphorylation and inactivation upon mitotic exit is triggered by PP1. *J. Cell Sci.* 129:1329–1339. https://doi.org/10.1242/jcs.178855

Machowska, M., K. Piekarowicz, and R. Rzepecki. 2015. Regulation of lamin properties and functions: does phosphorylation do it all? *Open Biol.* 5:150094. https://doi.org/10.1098/rsob.150094

Manchado, E., M. Guillamot, G. de Cárcer, M. Eguren, M. Trickey, I. García-Higuera, S. Moreno, H. Yamano, M. Cañamero, and M. Malumbres. 2010. Targeting mitotic exit leads to tumor regression in vivo: Modulation by Cdk1, Mastl, and the PP2A/B55α,δ phosphatase. *Cancer Cell.* 18:641–654. https://doi.org/10.1016/j.ccr.2010.10.028

Margalit, A., A. Brachner, J. Gotzmann, R. Foisner, and Y. Gruenbaum. 2007. Barrier-to-autointegration factor--a BAFfling little protein. *Trends Cell Biol.* 17:202–208. https://doi.org/10.1016/j.tcb.2007.02.004

Mayer-Jaekel, R.E., H. Ohkura, R. Gomes, C.E. Sunkel, S. Baumgartner, B.A. Hemmings, and D.M. Glover. 1993. The 55 kd regulatory subunit of Drosophila protein phosphatase 2A is required for anaphase. *Cell.* 72:621–633. https://doi.org/10.1016/0092-8674(93)90080-A

Mayer-Jaekel, R.E., H. Ohkura, P. Ferrigno, N. Andjelkovic, K. Shiomi, T. Uemura, D.M. Glover, and B.A. Hemmings. 1994. Drosophila mutants in the 55 kDa regulatory subunit of protein phosphatase 2A show strongly reduced ability to dephosphorylate substrates of p34cdc2. *J. Cell Sci.* 107:2609–2616.

McCloy, R.A., B.L. Parker, S. Rogers, R. Chaudhuri, V. Gayevskiy, N.J. Hoffman, N. Ali, D.N. Watkins, R.J. Daly, D.E. James, et al. 2015. Global Phosphoproteomic Mapping of Early Mitotic Exit in Human Cells Identifies Novel Substrate Dephosphorylation Motifs. *Mol. Cell. Proteomics.* 14:2194–2212. https://doi.org/10.1074/mcp.M114.046938

Mochida, S., S. Ikeo, J. Gannon, and T. Hunt. 2009. Regulated activity of PP2A-B55 delta is crucial for controlling entry into and exit from mitosis in Xenopus egg extracts. *EMBO J.* 28:2777–2785. https://doi.org/10.1038/emboj.2009.238

Mochida, S., S.L. Maslen, M. Skehel, and T. Hunt. 2010. Greatwall phosphorylates an inhibitor of protein phosphatase 2A that is essential for mitosis. *Science.* 330:1670–1673. https://doi.org/10.1126/science.1195689

Morgan, D.O. 2007. The Cell Cycle: Principles of Control. New Science Press, London. 297 pp.

Moutinho-Santos, T., P. Sampaio, I. Amorim, M. Costa, and C.E. Sunkel. 1999. In vivo localisation of the mitotic POLO kinase shows a highly dynamic association with the mitotic apparatus during early embryogenesis in Drosophila. *Biol. Cell.* 91:585–596. https://doi.org/10.1111/j.1768-322X.1999.tb01104.x

Nichols, R.J., M.S. Wiebe, and P. Traktman. 2006. The vaccinia-related kinases phosphorylate the N′ terminus of BAF, regulating its interaction with DNA and its retention in the nucleus. *Mol. Biol. Cell.* 17:2451–2464. https://doi.org/10.1091/mbc.e05-12-1179

Osouda, S., Y. Nakamura, B. de Saint Phalle, M. McConnell, T. Horigome, S. Sugiyama, P.A. Fisher, and K. Furukawa. 2005. Null mutants of Drosophila B-type lamin Dm(0) show aberrant tissue differentiation rather than obvious nuclear shape distortion or specific defects during cell proliferation. *Dev. Biol.* 284:219–232. https://doi.org/10.1016/j.ydbio.2005.05.022

Patterson, K., A.B. Molofsky, C. Robinson, S. Acosta, C. Cater, and J.A. Fischer. 2004. The functions of Klarsicht and nuclear lamin in developmentally regulated nuclear migrations of photoreceptor cells in the Drosophila eye. *Mol. Biol. Cell.* 15:600–610. https://doi.org/10.1091/mbc.e03-06-0374

Peter, M., J. Nakagawa, M. Dorée, J.C. Labbé, and E.A. Nigg. 1990. In vitro disassembly of the nuclear lamina and M phase-specific phosphorylation of lamins by cdc2 kinase. *Cell.* 61:591–602. https://doi.org/10.1016/0092-8674(90)90471-P

Rangone, H., E. Wegel, M.K. Gatt, E. Yeung, A. Flowers, J. Debski, M. Dadlez, V. Janssens, A.T. Carpenter, and D.M. Glover. 2011. Suppression of scant identifies Endos as a substrate of greatwall kinase and a negative regulator of protein phosphatase 2A in mitosis. *PLoS Genet.* 7:e1002225. https://doi.org/10.1371/journal.pgen.1002225

Rogers, S., R. McCloy, D.N. Watkins, and A. Burgess. 2016. Mechanisms regulating phosphatase specificity and the removal of individual phosphorylation sites during mitotic exit. *BioEssays.* 38(Suppl 1):S24–S32. https://doi.org/10.1002/bies.201670905

Ryder, E., M. Ashburner, R. Bautista-Llacer, J. Drummond, J. Webster, G. Johnson, T. Morley, Y.S. Chan, F. Blows, D. Coulson, et al. 2007. The DrosDel deletion collection: a Drosophila genomewide chromosomal deficiency resource. *Genetics.* 177:615–629. https://doi.org/10.1534/genetics.107.076216

Samwer, M., M.W.G. Schneider, R. Hoefler, P.S. Schmalhorst, J.G. Jude, J. Zuber, and D.W. Gerlich. 2017. DNA Cross-Bridging Shapes a Single Nucleus from a Set of Mitotic Chromosomes. *Cell.* 170:956–972.

Schellhaus, A.K., P. De Magistris, and W. Antonin. 2016. Nuclear Reformation at the End of Mitosis. *J. Mol. Biol.* 428(10, 10 Pt A):1962–1985. https://doi.org/10.1016/j.jmb.2015.09.016

Schmitz, M.H., M. Held, V. Janssens, J.R. Hutchins, O. Hudecz, E. Ivanova, J. Goris, L. Trinkle-Mulcahy, A.I. Lamond, I. Poser, et al. 2010. Live-cell imaging RNAi screen identifies PP2A-B55alpha and importin-beta1 as key mitotic exit regulators in human cells. *Nat. Cell Biol.* 12:886–893. https://doi.org/10.1038/ncb2092

Tekotte, H., D. Berdnik, T. Török, M. Buszczak, L.M. Jones, L. Cooley, J.A. Knoblich, and I. Davis. 2002. Dcas is required for importin-alpha3 nuclear export and mechano-sensory organ cell fate specification in Drosophila. *Dev. Biol.* 244:396–406. https://doi.org/10.1006/dbio.2002.0612

Thompson, L.J., M. Bollen, and A.P. Fields. 1997. Identification of protein phosphatase 1 as a mitotic lamin phosphatase. *J. Biol. Chem.* 272:29693–29697. https://doi.org/10.1074/jbc.272.47.29693

Uemura, T., K. Shiomi, S. Togashi, and M. Takeichi. 1993. Mutation of twins encoding a regulator of protein phosphatase 2A leads to pattern duplication in Drosophila imaginal discs. *Genes Dev.* 7:429–440. https://doi.org/10.1101/gad.7.3.429

Wang, P., X. Pinson, and V. Archambault. 2011. PP2A-twins is antagonized by greatwall and collaborates with polo for cell cycle progression and centrosome attachment to nuclei in drosophila embryos. *PLoS Genet.* 7:e1002227. https://doi.org/10.1371/journal.pgen.1002227

Wassarman, D.A., N.M. Solomon, H.C. Chang, F.D. Karim, M. Therrien, and G.M. Rubin. 1996. Protein phosphatase 2A positively and negatively regulates Ras1-mediated photoreceptor development in Drosophila. *Genes Dev.* 10:272–278. https://doi.org/10.1101/gad.10.3.272

White-Cooper, H., M. Carmena, C. Gonzalez, and D.M. Glover. 1996. Mutations in new cell cycle genes that fail to complement a multiply mutant third chromosome of Drosophila. *Genetics.* 144:1097–1111. https://doi.org/10.1534/genetics.112.1097.test

Williams, B.C., J.J. Filter, K.A. Blake-Hodek, B.E. Wadzinski, N.J. Fuda, D. Shalloway, and M.L. Goldberg. 2014. Greatwall-phosphorylated Endosulfine is both an inhibitor and a substrate of PP2A-B55 heterotrimers. *eLife.* 3:e01695. https://doi.org/10.7554/eLife.01695

Wlodarchak, N., and Y. Xing. 2016. PP2A as a master regulator of the cell cycle. *Crit. Rev. Biochem. Mol. Biol.* 51:162–184. https://doi.org/10.3109/10409238.2016.1143913

Wurzenberger, C., and D.W. Gerlich. 2011. Phosphatases: providing safe passage through mitotic exit. *Nat. Rev. Mol. Cell Biol.* 12:469–482. https://doi.org/10.1038/nrm3149

Yang, S.H., S.Y. Chang, L. Yin, Y. Tu, Y. Hu, Y. Yoshinaga, P.J. de Jong, L.G. Fong, and S.G. Young. 2011. An absence of both lamin B1 and lamin B2 in keratinocytes has no effect on cell proliferation or the development of skin and hair. *Hum. Mol. Genet.* 20:3537–3544. https://doi.org/10.1093/hmg/ddr266

Yuan, K., and P.H. O'Farrell. 2015. Cyclin B3 is a mitotic cyclin that promotes the metaphase-anaphase transition. *Curr. Biol.* 25:811–816. https://doi.org/10.1016/j.cub.2015.01.053

Zhuang, X., E. Semenova, D. Maric, and R. Craigie. 2014. Dephosphorylation of barrier-to-autointegration factor by protein phosphatase 4 and its role in cell mitosis. *J. Biol. Chem.* 289:1119–1127. https://doi.org/10.1074/jbc.M113.492777